

Article

Biodegradation of Choline NTF₂ by *Pantoea agglomerans* in Different Osmolarity. Characterization and Environmental Implications of the Produced Exopolysaccharide

Abrusci Concepción ^{1,2,*} , Amils Ricardo ^{1,2}  and Sánchez-León Enrique ¹ 

¹ Departamento de Biología Molecular, Facultad de Ciencias, Universidad Autónoma de Madrid, UAM, Cantoblanco, 28049 Madrid, Spain

² Centro de Biología Molecular Severo Ochoa, CSIC-UAM, 28049 Madrid, Spain

* Correspondence: concepcion.abrusci@uam.es; Tel.: +34-91-497-82-57

Abstract: A specific microorganism, *Pantoea agglomerans* uam8, was isolated from the ionic liquid (IL) Choline NTF₂ and identified by molecular biology. A biodegradation study was performed at osmolarity conditions (0.2, 0.6, 1.0 M). These had an important influence on the growth of the strain, exopolysaccharide (EPS) production, and biodegradation (1303 mg/L max production and 80% biodegradation at 0.6 M). These conditions also had an important influence on the morphology of the strain and its EPSs, but not in the chemical composition. The EPS (glucose, mannose and galactose (6:0.5:2)) produced at 0.6 M was further characterized using different techniques. The obtained EPSs presented important differences in the behavior of the emulsifying activity for vegetable oils (olive (86%), sunflower (56%) and coconut (90%)) and hydrocarbons (diesel (62%), hexane (60%)), and were compared with commercial emulsifiers. The EPS produced at 0.6 M had the highest emulsifying activity overall. This EPS did not show cytotoxicity against the tested cell line (<20%) and presented great advantages as an antioxidant (1,1-diphenyl-2-picryl-hydrazyl radical (DPPH) (85%), hydroxyl radical (OH) (99%), superoxide anion (O₂⁻) (94%), chelator (54%), and antimicrobial product (15 mm). The osmolarity conditions directly affected the capacity of the strain to biodegrade IL and the subsequently produced EPS. Furthermore, the EPS produced at 0.6 M has potential for environmental applications, such as the removal of hazardous materials by emulsification, whilst resulting in positive health effects such as antioxidant activity and non-toxicity.

Keywords: bacteria; ionic liquid; toxicity; emulsifying; antioxidant



Citation: Concepción, A.; Ricardo, A.; Enrique, S.-L. Biodegradation of Choline NTF₂ by *Pantoea agglomerans* in Different Osmolarity. Characterization and Environmental Implications of the Produced Exopolysaccharide. *Polymers* **2023**, *15*, 3974. <https://doi.org/10.3390/polym15193974>

Academic Editor: Shashi Kant Bhatia

Received: 31 August 2023

Revised: 24 September 2023

Accepted: 30 September 2023

Published: 3 October 2023



Copyright: © 2023 by the authors. Licensee MDPI, Basel, Switzerland. This article is an open access article distributed under the terms and conditions of the Creative Commons Attribution (CC BY) license (<https://creativecommons.org/licenses/by/4.0/>).

1. Introduction

Great industrial advances have allowed the development of many anthropogenic products with applications in many fields including industrial, agrochemical, pharmaceutical, food, and biotechnological [1–3]. These products are not exempt from causing serious problems for the environment and public health [4–7]. Ionic liquids (ILs) are a group of anthropogenic compounds that have been classed as “green” chemistry [8–10]. They are salts that, due to the nature of their composition, are formed by organic cations and a wide variety of organic and inorganic anions, allowing an infinite number of these compounds. Their exceptional properties, such as chemical and thermal stability, ionic conductivity, low vapor pressure, and high solvent power, among others, have made them an alternative to conventional solvents [11–13]. However, ionic liquids are not exempt from being able to cause problems in the environment [14,15]. This sparked a wave of new designs in the field of ionic liquids, the so-called third generation ionic liquids, intended to be safer for the environment where they were going to be implemented. Among these ionic liquids, those based on Choline should be highlighted. Their most desirable attributes, compared with other types of ionic liquids, were undoubtedly their biodegradable properties. Furthermore, they could be used in industrial processes such as CO₂ absorption [16,17], and very promisingly,

in biotechnology [18–20]. This, together with their low price, contributed decisively to the expansion of their usage. However, there are large gaps in the understanding of this type of choline-based ionic liquids, both in terms of their behavior in the aquatic environment and their cytotoxicity, since these are not yet extensively researched [21,22].

One strategy that can be used for the elimination of ionic liquids is bioremediation processes. The use of allochthonous microorganisms with the capacity to decontaminate these environments is the most environmentally friendly alternative. The use of microorganisms has, therefore, the advantage of being ecological, efficient, and economically very profitable. Previous work focused on the biodegradation of ILs [23–25] but not in the isolation of specific microorganisms from these compounds. Nor has the importance of the exopolysaccharides (EPSs) produced through IL biodegradation processes been deeply studied [26]. Therefore, there is a need to explore how these polymers can influence the environment where they are produced and their impact on the environment and public health [27,28]. The hypothesis is that the EPSs produced by specific microorganisms from the biodegradation of Choline NTF₂ under certain environmental conditions can directly influence the possible capacities of the EPSs by varying their emulsifying activity, chelating, and antioxidant activity, among others. The specific objectives of this research were the isolation and identification of specific microorganisms, the biodegradation of IL in different osmolarities and understanding the influence of the chemical composition, morphology, toxicity, and environmental relevance of the EPSs obtained. For this, a series of investigations were carried out to test this hypothesis. The strain *Pantoea agglomerans* uam8 was identified, the biodegradation of the IL was monitored through the production of CO₂ and the analysis of ion residues, and the EPS was characterized with different analytical techniques (transmission electron microscopy (TEM), scanning electronic microscopy (SEM), matrix-assisted laser desorption/ionization/time-of-flight (MALDI TOF), gas chromatography (GC–MS), high performance liquid chromatography–tandem mass spectrometry (HPLC–MS/MS), attenuated total reflectance/FT-infrared spectroscopy (ATR FTIR), thermogravimetric (TGA), and differential scanning calorimetric (DSC)). Furthermore, the applications of the EPSs were also studied including their bioremediation capabilities by monitoring their emulsifying activity and chelation properties. Additionally, cytotoxicity, morphology, reactive oxygen species and antimicrobial activity of the EPS were studied at a cellular level.

2. Materials and Methods

2.1. Materials

2.1.1. Chemicals

The compounds were supplied by different companies. The (2-Hydroxyethyl) trimethylammonium bis(trifluoromethylsulfonyl)imide Iolitec 99% Choline NTF₂ (IL) was obtained from IoLiTec Ionic Liquids Technologies GmbH (Heilbronn, Germany); the olive, sunflower, sesame, and coconut oils from Hipercor (Madrid, Spain); sephadex G-100 column from Aldrich Chemical Company, Inc. (Milwaukee, WI, USA); and trifluoroacetic acid (TFA) from Aldrich® (Schnelldorf, Germany). The following were purchased from Sigma-Aldrich (Madrid, Spain): diesel, hexane, toluene, dextrans standard, 1,1-diphenyl-2-picrylpolymers hydrazyl radical (DPPH), hydrogen peroxide (H₂O₂) 30%, salicylic acid 99%, pyrogallol, hydrochloric acid (HCl) 37%, potassium hydroxide (KOH), phosphate-buffered saline (PBS), hydrochloric acid (HCl) 37%, polyoxyethylene sorbitan monolaurate (Tween 20), sodium dodecyl sulphate (SDS), and 2-[4-(2,4,4-trimethylpentan-2-yl) phenoxy]ethanol (Triton X-100).

2.1.2. Microorganisms, Growth Assay, Cell Line and Storage

Trypticase soya agar (TSA), Luria–Bertani (LB), Dulbecco's modified Eagle's medium (DMEM) fetal bovine serum (FBS), L-glutamine, penicillin, streptomycin, catalase kit, and MTT (3-[4,5-dimethyl-thiazol-2-yl]-2,5-diphenyltetrazolium bromide) kit were obtained from Sigma-Aldrich (Madrid, Spain). *Escherichia coli* (*E. coli* CECT 516), *Staphylococcus*

aureus (*S. aureus* CECT 8753), *Enterococcus faecalis* (*E. faecalis* CECT 184), *Pseudomonas aeruginosa* (*P. aeruginosa* CECT 108), and *Salmonella typhimurium* (*S. typhimurium* CECT 409) were obtained from Colección Española de Cultivos (Spain). API 20E was obtained from BioMerieux España S.A. The HeLa cell line was purchased from CLS (Cell Line Service, Eppelheim, Germany). The UltraClean microbial DNA isolation kit was obtained from MO BIO Labs., Inc. (Solana Beach, CA, USA), and DNA purification JetQuick kit from Genomed (Leesburg, VA, USA).

2.2. Isolation and Identification of the Microorganism

A medium was prepared as described in Abrusci et al. [29] (MGM), g/L: K₂HPO₄ 0.5, KH₂PO₄ 0.04, NaCl 0.1, CaCl₂ 2H₂O 0.002, (NH₄)₂SO₄ 0.2, MgSO₄ 7H₂O 0.02, and FeSO₄ 0.001, and supplemented with glucose and Choline NTF₂ compound as a carbon source at the concentrations of 4 g/L and 50 mg/L, respectively. The media were exposed in the Universidad Autónoma de Madrid (Spain), with orientation 40°32'32.8" N/3°41'31.0" W for 72 h. Every 24 h, samples of 100 µL were taken and cultured in trypticase soya agar (TSA) and grown at 30 °C to isolate microorganisms. After the preliminary morphological and biochemical characterization, as used by Abrusci et al. [30], bacterial strains were identified using commercial identification kits. A commercial assay was employed: API 20E. The preparation and inoculation procedures followed the recommendations of the manufacturer with the strains being incubated at 30 °C for 24 h. The strain uam8 was amplified using polymerase chain reaction (PCR) and identified as undertaken by Morro et al. [31]. The universal 16 S rRNA gene primers 27 F (5'-AGAGTTTGATCCTGGCTCAG-3') and 1492 R (5'-GGTTACCTTGTTACGACTT-3') were used for PCR. The obtained sequences were compared with the sequences in NCBI GenBank using the Basic Local Alignment Search Tool (BLAST) (<https://blast.ncbi.nlm.nih.gov/Blast.cgi>). The selected sequences were aligned with CLUSTAL X [32].

2.3. Aerobic Biodegradation, Bacterial Growth, Microbial Cells, and pH. Analysis of Ion Residues Choline NTF₂

The aerobic biodegradation of the compound as a carbon source was prepared following the method described in Section 2.2, and the addition of NaCl (0.2 M/11.08 g/L, 0.6 M/35 g/L and 1.0 M/58.44 g/L) to strain uam8 was performed at 30 °C by indirect impedance measurements. The bioassays have been previously described in the literature [33]. These were performed in bioreactors filled with 1.5 mL of bacterial suspension. These were placed in plastic materials with 1.5 mL of 2 g/L of the aqueous KOH solution. The impedance was averaged on a Bac-Trac 4300 apparatus (SY-LAB Geräte GmbH). The percentage of biodegradation was calculated as a percentage of the ratio between the cumulative amount of CO₂ produced in the biodegradation at time, *t*, and the theoretical amount of carbon dioxide. Formula (1):

$$\% \text{ Biodegradation} = ([\text{CO}_2]_{\text{Prod}} / [\text{CO}_2]_{\text{Theor.}}) \times 100. \quad (1)$$

Bacterial growth was monitored with a spectrophotometer Biowave II+ (Biochrom Ltd.) to an optical density of 550 nm (OD₅₅₀ nm). Microbial cells were evaluated as a colony-forming unit (CFU) by different dilution plating incubated at 30 °C for 72 h with TSA agar medium. A Thermo Orion pH Meter (model, 2 Star) was used to determine the pH values during a period of 72 h [23]. The biodegradation of cation (Choline) and anion (NTF₂) was determined by high performance liquid chromatography–tandem mass spectrometry (HPLC–MS/MS) using an Agilent Technologies 1100 series—6410B (TQ). An ACE Excel 3 C18-Amide column as a stationary phase was used with a mobile phase of 0.1% formic acid in water. The flow rate was 0.2 mL/min. The temperature for analysis was set at 40 °C. Three independent assays were performed.

2.4. Production, Extraction and Purification of Exopolysaccharides

The strain was taken from the stock culture and inoculated in a trypticase soya agar medium (TSA). The plates were incubated at 30 °C for 24 h, after which the strain was transferred directly from the plate into flasks of 100 mL capacity filled with 20 mL of minimal growth medium prepared according to the method described in Section 2.2 plus NaCl (0.2, 0.6 and 1.0 M). The flasks were incubated in a rotary shaker incubator (Biogen) at 30 °C and 110 rpm for 72 h. After the first incubation, 10 mL of this broth (2.5×10^7 cells/mL concentration) was inoculated into flasks of 1000 mL capacity filled with 100 mL of this medium. The flasks were incubated at 30 °C and 110 rpm for 72 h, at which time the stationary phase was reached. Three independent assays were performed. The cultures obtained from the uam8 strain were centrifuged at $13,154 \times g$ for 30 min at 4 °C Duppont—RC5 [34]. The EPS was precipitated with three volumes of ethanol. This was collected by centrifugation and dissolved in Milli-Q water. Subsequently, it was dialyzed at 4 °C with Milli-Q water for 48 h. Finally, it was lyophilized, and the dry weight was determined. A DEAE-52 anion exchange column (2.6 × 30 cm) was used to determine the purification of the EPS. Deionized water was used for elution and NaCl (0.2–1.5 M) as eluent at a flow rate of 1 mL/min, using the phenol-sulfuric acid method. The fractions were collected and lyophilized, and the EPS was obtained.

2.5. Transmission Electron Microscopy (TEM) Analysis and Scanning Electronic Microscopy (SEM)

TEM studies were undertaken to study the influence of Choline NTF₂ over the uam8 strain [35]. The specimens were prepared by putting ca. 5 µL of a 0.05 wt % solution on a TEM copper grid with carbon support film (200 mesh, CBMSO, Madrid, Spain), and observed using a JEOL JEM-1200 (JEOL GmbH) at 120 kV. All images were recorded digitally with a bottom-mounted 4*4k CMOS camera (TemCam-F416, TVIPS).

Scanning electronic microscopy (SEM) studies were undertaken to investigate the exopolymers produced by the uam8 strain both with and without Choline NTF₂. The micrographs were obtained using a Philips XL 30 scanning electron microscope operating in a conventional high-vacuum mode at an accelerating voltage of 25 kV. Previously, EPS was coated with a 3 nm thick gold/palladium layer [36].

2.6. Exopolysaccharide Molecular Weight and Monosaccharides Identification

The molecular weight of EPS was obtained by matrix-assisted laser desorption/ionization/time-of-flight (MALDI TOF/TOF) analyzer equipped with a Nd:YAG 355-nm laser (Ultraflex III, Bruker) as described previously [34]. Mass spectra were recorded in positive reflector (range 1–10 KDa) and lineal (range 1–20 KDa) modes, using a matrix of 10 mg/mL 2,5-dihydroxybenzoic acid (DHB) in methanol/water (90/10).

Gas chromatography (EVOQ GC-TQ, Bruker) coupled with a mass spectrometry detector (GC-MS) was used to determine monosaccharides following the procedure described in the literature [37]. EPS was hydrolyzed at 120 °C for 2 h with 0.5 M trifluoroacetic acid (TFA). A 1 µL sample with source temperature of 230 °C was injected into the capillary column (30 m × 0.250 mm) and gas helium (1 mL/min). Glucose, arabinose, rhamnose, xylose, mannose, galactose, fructose and sorbose were used as standard. HPLC-MS/MS using an Agilent Technologies 1100 series was used for the determination of amino acids and glucuronic acid [38]. For this, the ACE Excel 3 C18-Amide column (stationary phase) and 0.1% formic acid in water (mobile phase) were used. Flow temperature was 0.2 mL/min at 40 °C.

2.7. Attenuated Total Reflectance/FT-Infrared Spectroscopy (ATR FTIR). Thermogravimetric (TGA) and Differential Scanning Calorimetric (DSC) Analysis

The IR spectra of EPS for the determination of the structural functional groups [31] were obtained using a Perkin Elmer BX-FTIR spectrometer coupled with an ATR accessory, MIRacle™-ATR from PIKE Technologies. Thermogravimetric analysis (TGA) of the EPS (1–3 mg) was performed using a TGA Q-500 (Perkin-Elmer). The heating rate for the

dynamic conditions was 10 °C/min, and the nitrogen flow was maintained at a constant rate of 60 mL/min. DSC measurements with the EPS (0.5–2 mg) were performed using a DSC Q100 (TA Instruments). The cuvettes were heated (20 to 600 °C) at a rate of 10 °C/min. Data were analyzed using the TA Universal Analysis software [39].

2.8. Emulsifying Activity

The emulsifying capabilities of the exopolymers was evaluated using the procedure described in [40]. The assays were undertaken in transparent cylindrical 5 mL tubes which contained 1.5 mL of an oil phase and 1.5 mL of an aqueous phase. The oil phase contained vegetable oils (olive sunflower, sesame, and coconut) and hydrocarbons (diesel, hexane, toluene). For the aqueous phase, both commercial emulsifying compounds (such as polysorbate (Tween 20), sodium dodecyl sulfate (SDS), Triton X-100), and the obtained EPS were used for comparison purposes. All compounds used had a concentration 3:2 *v/v*. The tubes were stirred in a vortex at 2400 rpm for 2 min. After 24, 168 h, the emulsification index (E24, E168) was determined as follows by Formula (2):

$$E_{24\text{ h}} = \text{HEL}/\text{HT} \times 100 \quad (2)$$

where HEL (mm) is the height of the emulsion layer and HT (mm) is the overall height of the mixture. The emulsion formation and stabilization were also assessed.

2.9. Nonenzymatic Antioxidants Assays

Nonenzymatic antioxidants assays for 1,1-diphenyl-2-picryl-hydrazyl radical (DPPH•), hydroxyl radical (•OH), and superoxide anion ($\text{O}_2^- \bullet$) were evaluated as indicators of the free radical scavenging activities of the EPS at different concentrations (0.1, 0.25, 1.0, 2.5, 5.0, 7.5 and 10 mg/mL). The tests were carried out following the calculations and the procedure described in Sánchez-León et al. [37]. The DPPH assay was carried out with different concentrations of EPS (50 µL) that were mixed with 100 µL of DPPH (100 µM DPPH–ethanolic solution). The mixture was incubated at 25 °C for 30 min.

The OH assay was performed with the EPS diluted to various concentrations (40 µL) which were mixed with 40 µL of 9 mM ethanol-salicylic acid solution, FeSO_4 solution (9 mM, 40 µL), and H_2O_2 (8.8 mM, 40 µL). The O_2^- assay was effected with different concentrations of EPS (0.3 mL) which were mixed with 2.6 mL of phosphate buffer (50 mM, pH 8.2) and 90 µL of pyrogallol (3 mM), dissolved in HCl (10 mM). Absorbances were measured using a FLUOstar Omega spectrophotometer (DPPH/ $\text{OD}_{525\text{ nm}}$), (OH/ $\text{OD}_{510\text{ nm}}$) and (O_2^- / $\text{OD}_{325\text{ nm}}$). Ascorbic acid (Vc) was used as a positive control.

$$\text{DPPH/OH Radical Scavenging Activity [\%]} = [1 - (A_1 - A_2)/A_0] \times 100 \quad (3)$$

Formula (3) was used to determine the percentage of radical-scavenging activity for DPPH, where A_1 represents the reaction mixture, A_2 refers to the reaction mixture without DPPH, and A_0 denotes the reaction mixture with DPPH and without EPS.

Formula (3) was used to determine the percentage of radical-scavenging activity for OH, where A_1 represents the reaction mixture, A_2 refers to the reaction mixture without salicylic acid, and A_0 denotes the reaction mixture with salicylic acid and without EPS.

$$\text{Superoxide scavenging activity [\%]} = 1 - (A_{10}/C_{10}) - (A_0/C_0) \times 100 \quad (4)$$

Formula (4) was used to determine the percentage of superoxide scavenging activity ($\text{O}_2^- \bullet$), where A_0 and A_{10} represent the reaction mixture at 0 and 10 min, respectively; C_0 and C_{10} represent the reaction mixture without pyrogallol at 0 and 10 min, respectively.

2.10. Toxicity Assay

Toxicity assay was determined using the MTT (3-[4,5-dimethyl-thiazol-2-yl]-2,5-diphenyltetrazolium bromide) test (Sigma Aldrich) on HeLa cells. The toxicity of the

EPS was tested at different concentrations (0–400 µg/mL) for 24 h, by the reduction of the MTT reagent to formazan as described by Perez-Blanco et al. [41]. HeLa cells were seeded in a 24-well culture plate (5×10^5 cells/mL). The OD_{590 nm} (FLUOstar Omega spectrophotometer) was recorded using a microplate reader.

2.11. Measurement of the Non-Radical H₂O₂, Morphological Cell and Catalase (CAT) Assay

2.11.1. Measurement of the Non-Radical H₂O₂

Damage Inducement

The methodology used to measure the damage of the non-radical H₂O₂ on HeLa cells was based on the procedure described by Huang-lin et al. [38]. For this, the cells were seeded at a density of 5×10^4 cells per well for 24 h. The medium was removed and replaced with 100 µL of H₂O₂ (0.25–2 mM) for 1 h at 37 °C, which was removed after this time. Cell viability was measured using the MTT method as described in Section 2.10.

HeLa cell viability was computed using Formula (5):

$$\text{Cell viability (\%)} = (A_1/A_2) \times 100 \quad (5)$$

where A_1 represents the absorbance of HeLa cells treated with H₂O₂ and the MTT solution, while A_2 represents the absorbance of HeLa cells that were not subjected to any treatment with the MTT solution.

Protective Effect of EPS against Non-Radical H₂O₂

The ability of EPS to protect HeLa cells against the non-radical H₂O₂ was evaluated following the method described by Huang-lin et al. [38]. For this, the cells were seeded at a density of 5×10^4 cells per well for 24 h. DMEM solutions were removed and replaced by EPS diluted in DMEM at different concentrations (25–400 µg/mL) for 1 h. They were removed and 2 mM H₂O₂ was added and incubated for 1 h. The MTT method described in Section 2.10 was used to determine cell viability. As a positive control, ascorbic acid (20 mg/mL) was used.

HeLa cell viability was calculated with Formula (6):

$$\text{Cell viability [\%]} = (A_1/A_2) \times 100 \quad (6)$$

where A_1 refers to cells that were treated with both H₂O₂ and EPS, and subsequently exposed to the MTT solution; and A_2 refers to cells that did not receive any treatment and were exposed to the MTT solution.

2.11.2. Morphological Cell

Cell morphology was determined using an Olympus CKX53 fluorescence microscope with a DAPI filter. The same procedure as that performed with the measurement of the non-radical H₂O₂ was carried out. All images were captured with a 10x objective and analyzed with Olympus DP-23 software (Olympus Corporation, JPN).

2.11.3. Catalase (CAT) Assay

The protective capacity of the EPS against oxidative stress was investigated using HeLa cells [42]. A total of 5×10^5 HeLa cells were seeded in 24-well plates and incubated for 24 h. The medium was subsequently discarded, and the cells were washed with phosphate-buffered saline (PBS). Then, cells were treated with EPS at various concentrations (50, 100, 200, and 400 µg/mL) that were dissolved in PBS and incubated for 1 h at 37 °C. Once the treatment had elapsed, the supernatants were collected and used for the determination of CAT. This activity was determined using a test kit (Catalase assay Kit from sigma) according to the protocol.

2.12. Chelating Activity

The chelating capacity of metals was carried out following the calculations and the operational procedure tested by Huang-lin et al. [38] against ferrous ions using ferric nitrate at two different pH values of the final reaction mixture (2.5 and 5.6). The mixture was prepared with 1.0 mL of EPS (0.1 to 10 mg/mL), 0.05 mL of FeCl₂ (2 mM), 0.2 mL of ferrozine (5 mM), and 2.75 mL of Milli-Q water and incubated at room temperature for 10 min. Ethylenediaminetetraacetic acid (EDTA) was used as a positive control. An OD_{562 nm} (FLUOstar Omega spectrophotometer) was used.

The chelating ability on ferrous ion was calculated according to Formula (7):

$$\text{Chelating ability [\%]} = [(A_0 - (A_1 - A_2)/A_0)] \times 100 \quad (7)$$

where,

A₀ = OD_{562nm} of the deionized water.

A₁ = OD_{562nm} of the reaction mixture.

A₂ = OD_{562nm} of the reaction mixture but without FeCl₂.

2.13. Antibacterial Activity by Agar Well Diffusion Assay

Agar well diffusion assay was used to evaluate the antibacterial activity of EPS following the method reported by Rajoka et al. [43]. The *E. coli* CECT 516, *Staphylococcus aureus* CECT 8753, *Enterococcus faecalis* CECT 184, *Pseudomonas aeruginosa* CECT 108, and *Salmonella typhimurium* CECT 409 strains were used as indicator microorganisms to evaluate the antibacterial activity of EPS. The plates prepared with the Luria–Bertani (LB) medium were inoculated with 100 µL of bacterial suspension (10⁷ CFU/mL). Wells (4 mm in diameter) were made, where 60 mL of EPS was deposited at different concentrations (1–10 mg/mL). The LB agar plates were kept at 4 °C for 1 h and incubated at 30 °C for 24 h. The antimicrobial activity was determined by measuring the diameter of the inhibition zone around the wells.

2.14. Statistical Analysis

Analysis of variance test (ANOVA) was performed to undertake the statistical comparisons by using the Statistical Package for the Social Sciences version 21 (SPSS® Inc., Chicago, IL, USA). *p* < 0.05 was considered statistically significant.

3. Results and Discussion

3.1. Isolation of Bacterial Strain, Morphological and Biochemical Characterization

The strain, uam8, was isolated as described in Section 2.2 using Choline NTF₂ as the only carbon source (Figure 1a). The bacterial strain was identified by means of its 16S rDNA sequence obtained after PCR amplification and sequencing. Comparison of the 16S rDNA sequences of the isolated strain with the available sequences in the GenBank database showed that the isolated bacteria was *P. agglomerans* uam8, with a similarity of 100% to MH101508.1. It is a bacterium that belongs to the family of Enterobacteriaceae [44]. Typically, *P. agglomerans* occupies different ecological niches. Therefore, this species is widely distributed in soils, water, plants, animals and humans [45].

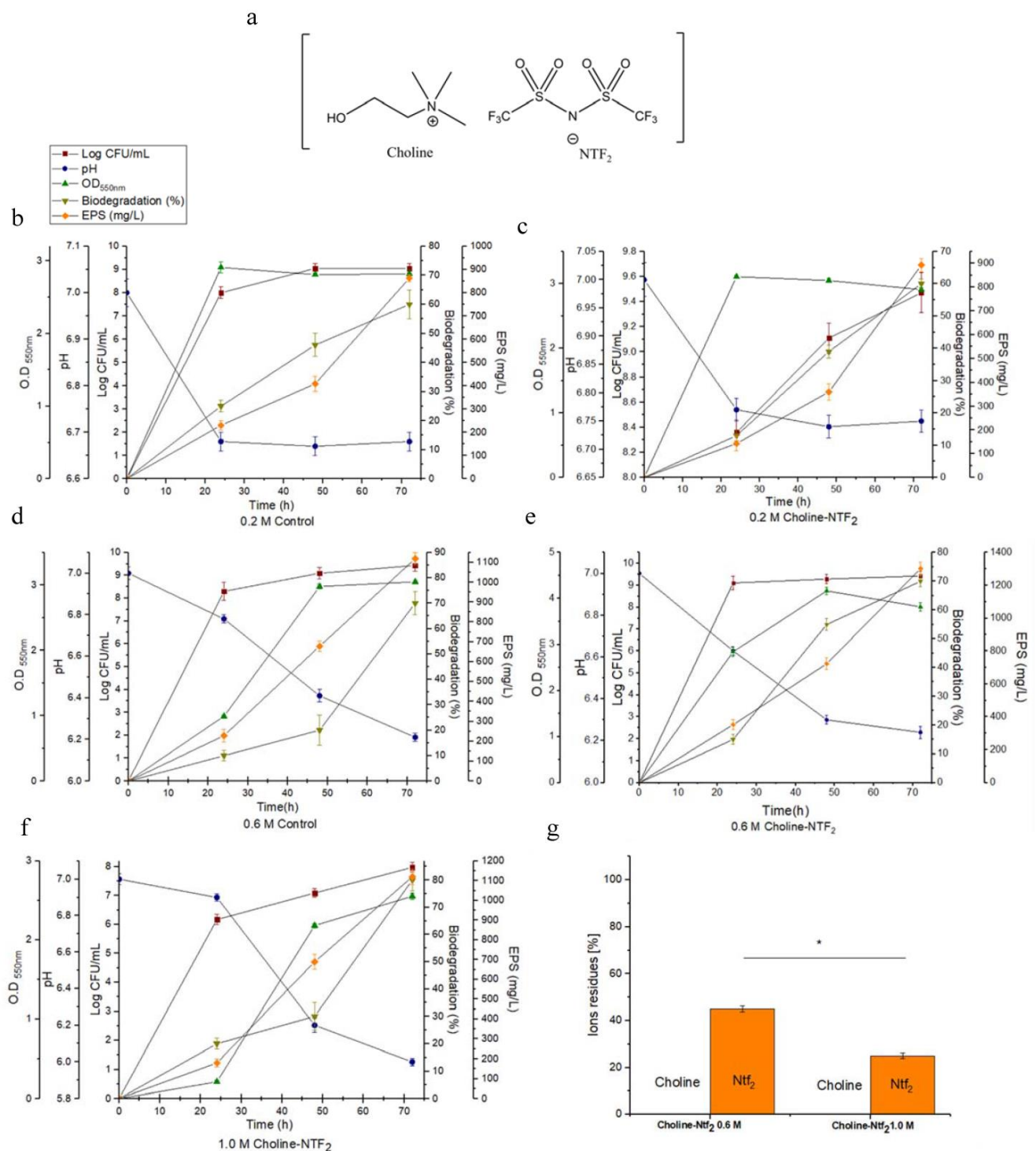


Figure 1. (a) Structural representation of the ionic liquid Choline NTF₂. Optimization of the production of EPS at different saline concentrations and Choline NTF₂ presence; (b) 0.2 M control; (c) 0.2 M Choline NTF₂; (d) 0.6 M control; (e) 0.6 M Choline NTF₂; (f) 1.0 M Choline NTF₂; (g) detection of ionic liquid (Choline NTF₂) after biodegradation. * ($p < 0.05$).

The results of the morphological and biochemical tests indicated that the strain *P. agglomerans* uam8 was a Gram-negative bacillus with motility, negative oxidase, positive catalase, and facultative anaerobic characteristics. It did not produce H₂S and did not hydrolyze the gelatin. It was found to be capable of fermenting a great number of compounds except for sorbitol and inositol and was not sensitive to streptomycin. These morpho-

logical and biochemical characteristics are mostly shared among the different strains of *P. agglomerans* [46,47]. In addition to this, even within the different species of the genus, there is a pattern of similarity of these characteristics, such as in the species of *P. vagans* [48], *P. gaviniae* [49], and *P. annatis* [50].

3.2. Monitoring of Growth and Biodegradation Parameters. Production of Exopolysaccharides

The experiments (Figure 1) were conducted using both glucose (control) and glucose with an IL (Choline NTF₂) (Figure 1a) in different osmotic conditions (0.2, 0.6, 1.0 M), during a period of 72 h and at a temperature of 30 °C. The influence that these parameters had on bacterial growth was measured in colony-forming units (CFU), pH, exopolymer production and biodegradation evaluated by indirect impedance measurements. In 0.2 M osmolarity conditions there were no significant differences in growth of *Pantoea agglomerans* uam8 between the control, (0.2 M Control/2.82 ± 0.06) (Figure 1b) and the presence of the IL (0.2 M Choline NTF₂/2.91 ± 0.04) (Figure 1c) in the studied period. However, with an osmolarity of 0.6 M, the presence of the IL increased bacterial growth (0.6 M Choline NTF₂/4.168 ± 0.06) (Figure 1e) with respect to the control (0.6 M Control/3.05 ± 0.03) (Figure 1d). With an osmolarity of 1.0 M, the presence of only glucose (1.0 M Control) did not result in any bacterial growth, however this occurred when the IL was present (1.0 M Choline NTF₂/2.554 ± 0.04) (Figure 1f). In the results, a larger number of CFUs were observed when the IL was present across all studied osmolarities (0.2 M Choline NTF₂/9.43 ± 0.2), (Figure 1c); (0.6 M Choline NTF₂/9.47 ± 0.3), (Figure 1e); and (1.0 M Choline NTF₂/7.98 ± 0.17), (Figure 1f). For 0.6 M Choline NTF₂ (pH 7 to just 6.4) (Figure 1e), no acute pH descent was detected, as the acidification of the medium was very low. However, for all other studied conditions, the pH decreased until 6 as was the case of 1.0 M Choline NTF₂, where the medium was acidified (Figure 1f). pH would be an important factor to take into account in high molarities. It was also observed that the presence of the IL at 0.6 M resulted in the largest production of the exopolymer (0.6 M Choline NTF₂/1303 mg L⁻¹) (Figure 1e), compared with (0.2 M Choline NTF₂/900 mg L⁻¹) (Figure 1c) and (1.0 M Choline NTF₂/1100 mg L⁻¹) (Figure 1f). In the case of *Pantoea* sp [51], high levels of EPS production were associated with environmental stress, caused by high salt concentrations. However, in other cases such as *Volcaniella eurihalina* (0.8 mg L⁻¹) [52], *Kocuria rosea* ZJUQH (2008 mg L⁻¹) [53], and *Lactobacillus confuses* (25,960 mg L⁻¹) [54], the higher production of EPS did not have a direct relationship with high saline concentrations. In our study, this production seems to be associated with the use of the choline cation. The presence of a nitrogen source favored both the growth rate and the production of EPS [55]. The results also indicated that the largest efficiency in the biodegradation of the carbon sources (80%) was reached when both sources (glucose and IL) were available together and at high molarity, at 0.6 M Choline NTF₂ (Figure 1e) and 1.0 M Choline NTF₂ (Figure 1f). On the other hand, the analysis of the ions that comprise the IL confirmed that both ions were used by the strain in conditions of high osmolarity (0.6 M Choline NTF₂ and 1.0 M Choline NTF₂) (Figure 1g), but in an unequal way. The cation (choline) was not residual, which confirms the use of this by the strain. This indicated that the entry of choline into the cell was carried out successfully, showing that this process was dependent on the salinity of the environment [56]. The entry of choline into the cell could be mediated by ABC-type transporters driven by a proton-sodium gradient. Once inside, the transformation from choline to glycine betaine took place which had an osmoprotective effect on the strain [57]. This favored the adaptation of the strain to saline environments [58]. This adaptation translated into higher rates of cell growth [59] and EPSs production [51]. For the anion (NTF₂), its biodegradation was independent of the choline cation. Under the conditions of 0.6 M Choline NTF₂, 42% of the anion was residual, whereas for 1.0 M Choline NTF₂, only 25% of the anion was residual. These results confirmed a larger utilization by *P. agglomerans* uam8 of the anion (NTF₂) at a higher osmolarity. This could be because the high concentration of sodium chloride favored the solubility of the anion and its bioavailability. Gram-negative bacteria (*Sphingomonas*,

Pseudomonas and *P. agglomerans*) have been effective in biodegrading toxic compounds such as phosphonium-based ILs [60,61] and chlorinated hydrocarbons (85%) [62].

3.3. Transmission Electron Microscopy (TEM) and Scanning Electron Microscopy (SEM)

TEM studies were undertaken (Figure 2) to investigate the possible changes that occurred at high osmolarity in bacterial cells both in 0.6 M Control and in the presence of the IL 0.6 M Choline NTF₂, in the first 24 h. With 0.6 M Control (Figure 2a), the cells presented a contracted cytoplasmic volume with loss of turgor. However, in the 0.6 M Choline NTF₂ medium, the cells presented a turgid appearance and without any deformations (Figure 2b,c). This revealed that *P. agglomerans* uam8 in the absence of Choline NTF₂ could not synthesize into glycine betaine through novo synthesis, and the cells were damaged. However, when the bacteria were grown with choline, cell turgor was maintained due to the conversion of Choline NTF₂ into glycine betaine. This suggests that this strain may have environmental applications in Choline NTF₂ bioremediation. Similar results were found in *B. subtilis* [63,64], and *Tetragenococcus halophila* [65] which required the presence of choline to produce glycine betaine.

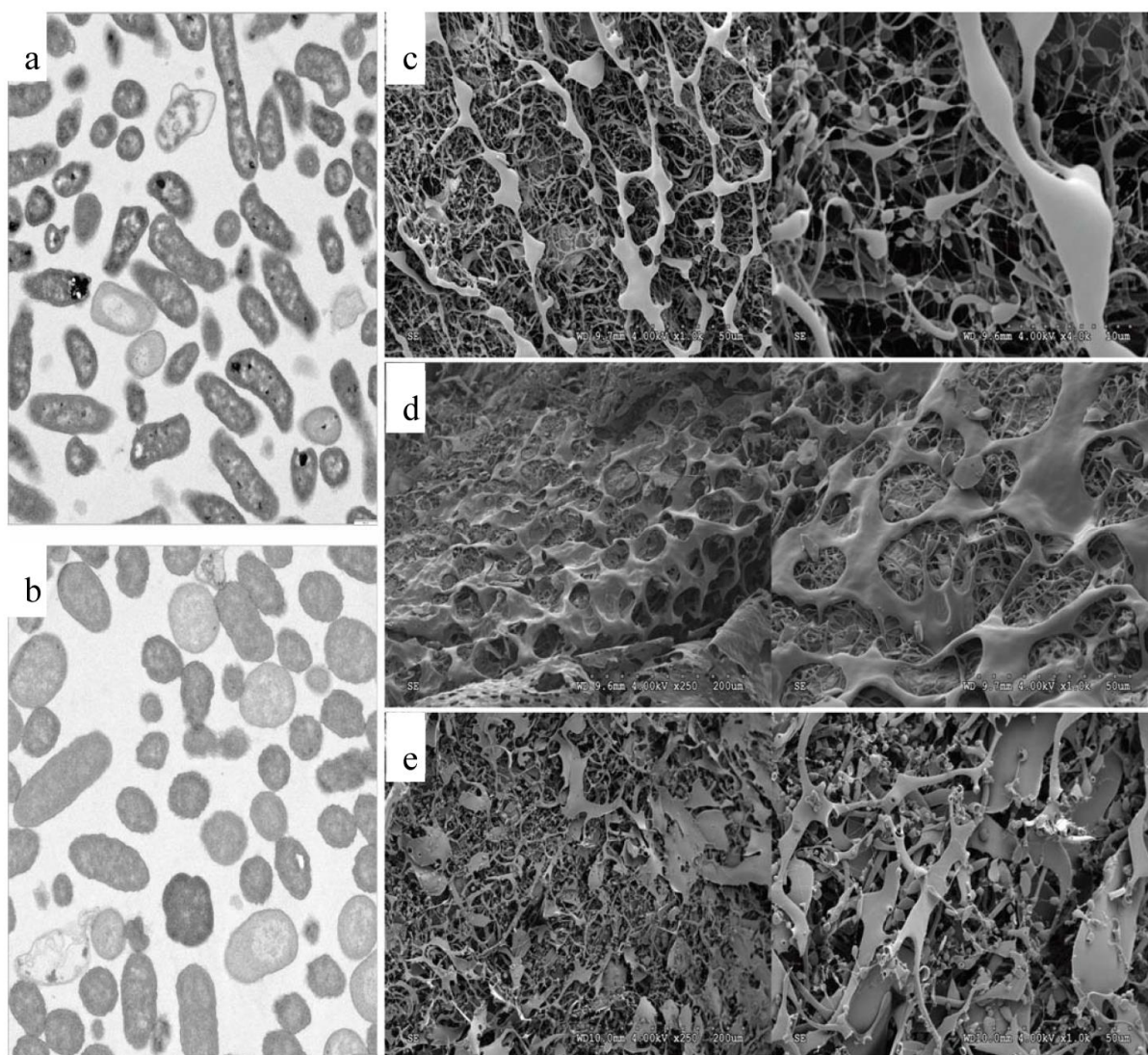


Figure 2. Electron microscopy: (a) TEM of cell on 0.6 M Control, (b) TEM of cell on 0.6 M Choline NTF₂, (c) SEM of EPS to 0.6 M Control, (d) SEM of EPS to 0.6 M Choline NTF₂, (e) SEM of EPS to 1.0 M Choline NTF₂.

The SEM study revealed that the obtained EPSs at 0.6 M Control (Figure 2d), 0.6 M Choline NTF₂ (Figure 2e), and 1.0 M Choline NTF₂ (Figure 2e) presented morphological differences between them. The EPS obtained from 0.6 M Control and 1.0 M Choline NTF₂ presented a greater number of finely filamentous structures. However, the EPS obtained from 0.6 M Choline NTF₂ presented broader structures. These differences were due to the osmolarity conditions and the absence or presence of Choline NTF₂. Similar results were found in the EPSs of *Shewanella oneidensis* strain MR-1 [66] and *Bacillus pseudomycooides* U10 [67]. This indicated that the morphology of the polymers was affected by environmental and nutritional conditions.

3.4. Characterization of the Exopolysaccharides

The EPS produced from the biodegradation of 0.6 M Choline NTF₂ was characterized, because it was under these conditions where the highest EPS production took place and its morphology was the least damaged. In addition, the osmolarity conditions were adjusted to those typical of seawater salinity (35 g/L), which made for more interesting environmental conditions.

The EPS produced from the biodegradation of 0.6 M Choline NTF₂ presented an isolated peak, Figure 3a. On the other hand, the other EPSs produced in this study (0.2 M Choline NTF₂, and 1.0 M Choline NTF₂) also presented this characteristic. This highlighted that the obtained polymers were pure. This is an important feature of bacterial exopolysaccharides [38]. The mass spectrum of the purified EPS of 0.6 M Choline NTF₂ showed a molecular weight of 5221.5 Da. (Figure 3b). This low molecular weight that this EPS presented was due to the osmotic conditions. Extreme environmental conditions can give rise to low molecular weight EPSs, as was the case of the EPS produced by *Synechococcus* PCC7942, with a molecular weight of 3–10 KDa [68].

The EPS produced by *P. agglomerans* uam8 from biodegrading 0.6 M Choline NTF₂ was analyzed by gas chromatography GC–MS Figure 3c. EPS was a heteropolysaccharide, exclusively composed of three monosaccharides, glucose (α -glucose, β -glucose), galactose and α -mannose, with a molar ratio of 6:2:0.5, respectively. The presence of the glucose monomer as a component of these EPSs seems recurrent in the genus *Pantoea*. Preliminary investigations have supported this fact. The *Pantoea agglomerans* strain [69] showed an EPS formed by a heteropolysaccharide that contained mannose and glucose in a ratio of 3:2. This EPS was obtained from glucose and yeast as a carbon source. *Pantoea* sp. (BM39) [51,70] produced an EPS that was a homopolysaccharide, formed exclusively from glucose, from sucrose, glucose and fructose as a carbon source.

Less common monomers such as the heteropolysaccharide of *Pantoea* sp. have also been described in the EPSs of the genus *Pantoea* YU16-S3 [71] with glucose, galactose, N-acetyl galactosamine, and glucosamine in the ratio of 1.9:1:0.4:0.02, respectively. This EPS was obtained from a marine environment, containing peptone and yeast. Some of these clear differences in the compositions of the EPSs can be attributed to genetic and physiological factors.

FT-IR spectroscopy is an analytical technique that allows the identification of functional groups from absorption peaks [72]. The FT-IR spectrum of EPS from 0.6 M Choline NTF₂ is shown in Figure 4a. In addition, the FTIR spectra of all the other EPSs produced in this study (0.2 M Choline NTF₂, 0.6 M Control and 1.0 M Choline NTF₂), shown in Figure 4a, revealed a broad homology between the EPSs samples. This demonstrated that neither the nutritional nor the environmental factors conditioned the composition of the EPS. The broad and strong peak of 3292 cm⁻¹ and 2928 cm⁻¹ indicated O-H stretching vibration and C-H stretching vibration, respectively [73,74]. The peak at 1600 cm⁻¹ and 1401 cm⁻¹ was attributed to the ionic carboxyl group (COO⁻) and C-H bond vibration, respectively [75]. According to a previous study, the absorption at 1246 cm⁻¹ could be attributed to the pyranose ring [37]. Absorption peaks in the 1160 cm⁻¹ region indicated C–O–C stretching vibration and the peak at 1018 cm⁻¹ was due to C–O–H stretching vibration [76]. FT-IR spectroscopy of the EPS was characteristic of the presence of polysaccharides in the EPS.

These groups were also present in the EPS of other strains of *Pantoea agglomerans* [69], and in *Pantoea alhagi* NX-11 [77].

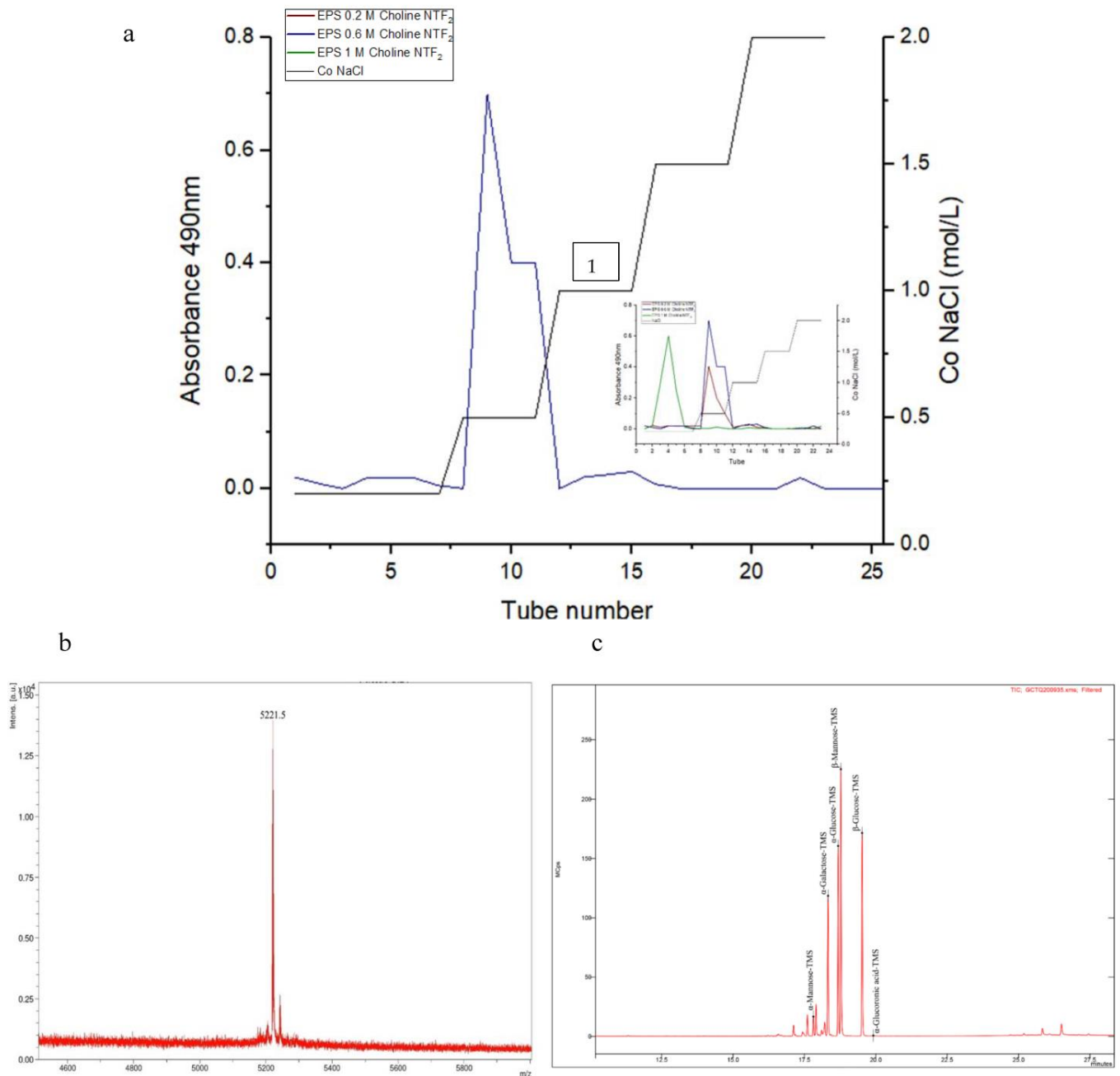


Figure 3. Characterization of the exopolymer EPS extracted from *Pantoea agglomerans*: (a) elution curve obtained from the purification of EPS 0.6 M Choline NTF₂, and (1) of EPS 0.2 M Choline NTF₂ and 1.0 M Choline NTF₂; (b) MALDI-TOF mass spectroscopy of EPS 0.6 M Choline NTF₂; (c) GC-MS of EPS 0.6 M Choline NTF₂.

One of the important factors to take into account for an efficient environmental application of bacterial exopolysaccharides is the study of their thermal stability. The TGA analysis showed (Figure 4b) that the EPS (0.6 M Choline NTF₂ medium) experienced an initial weight loss of 11.04% due to moisture content at approximately 180 °C. This is due to the carboxyl groups of the polysaccharide, which have an affinity for water molecules. Subsequently, a weight loss of around 61% occurred at 365 °C, which was attributed to the degradation of the sample itself. Furthermore, the DSC analysis (Figure 4c) of this sample

showed two melting peaks at 317.22 °C and 444.51 °C. The degradation temperature of the purified EPS of 0.6 M Choline NTF₂ was lower than the purified EPS from *Pantoea* sp. BCCS 001 GH (weight loss (69%) at 318 °C) [78,79] and *Pantoea* sp. YU16-S3 (weight loss (20%) at 200 °C) [71], which contained different monosaccharides in their EPSs. These differences could be decisive in thermal stability and, therefore, in its environmental and industrial application.

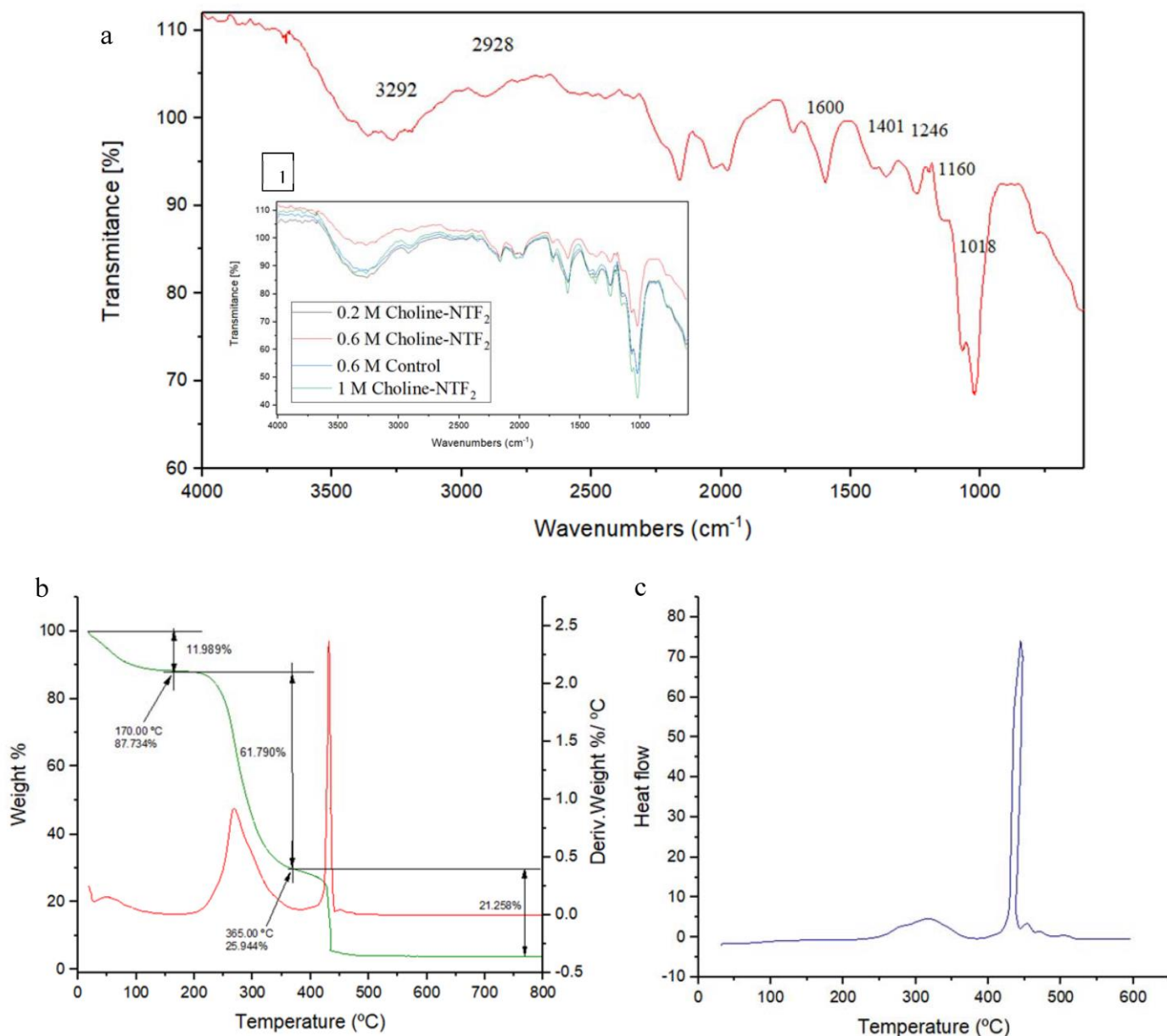


Figure 4. (a) ATR–FTIR of EPS 0.6 M Choline NTF₂ and EPS produced (1) by 0.2 M Choline–NTF₂, 0.6 M Control and 1.0 M Choline–NTF₂. (b) TGA of EPS 0.6 M Choline NTF₂. (c) DSC of EPS 0.6 M Choline NTF₂.

3.5. Environmental Implications of the Produced Exopolysaccharides

3.5.1. Emulsifying Study

The emulsifying activity of the exopolysaccharides is crucial for its environmental application. This activity is determined by measuring the retention of the emulsion of vegetable oils or hydrocarbons in water after a certain time period. The EPS (0.6 M Choline NTF₂ medium) emulsification study was carried out at different times (24 h (E24) and 168 h

(E168)), concentrations (0.5, 1, and 2 mg/mL), and at pH 7.0, and with both vegetable oils (olive, sunflower, sesame, and coconut) and hydrocarbons (diesel oil, hexane, toluene).

Figure 5a shows the effectiveness of EPS as an emulsifier for the studied vegetable oils. The results indicated that for 24 and 168 h, the effectiveness of EPS as an emulsifier of vegetable oils was not effective at the concentrations of 0.5 and 1 mg/mL. Emulsification percentages of more than 50% were not reached for any of them. In the concentration of 2 mg, for 24 h ($p < 0.05$), high emulsification values were given for olive oil ((E24) 86.4%), sunflower oil ((E24) 56%), and coconut oil ((E24) 90%). However, for 168 h, the activity was only maintained for coconut oil ((E168) 90%). Figure 5b shows the effectiveness of EPS as an emulsifier for hydrocarbons. The emulsification was effective at 1 mg/mL only for diesel ((E24) 60%), and at 2 mg/mL for diesel ((E24) 62%) and hexane ((E24) 60%). For 168 h, the emulsifying activity was maintained only for diesel, in concentrations of 1 mg/mL and 2 mg/mL ((E168) 57%), ((E168) 61%), respectively.

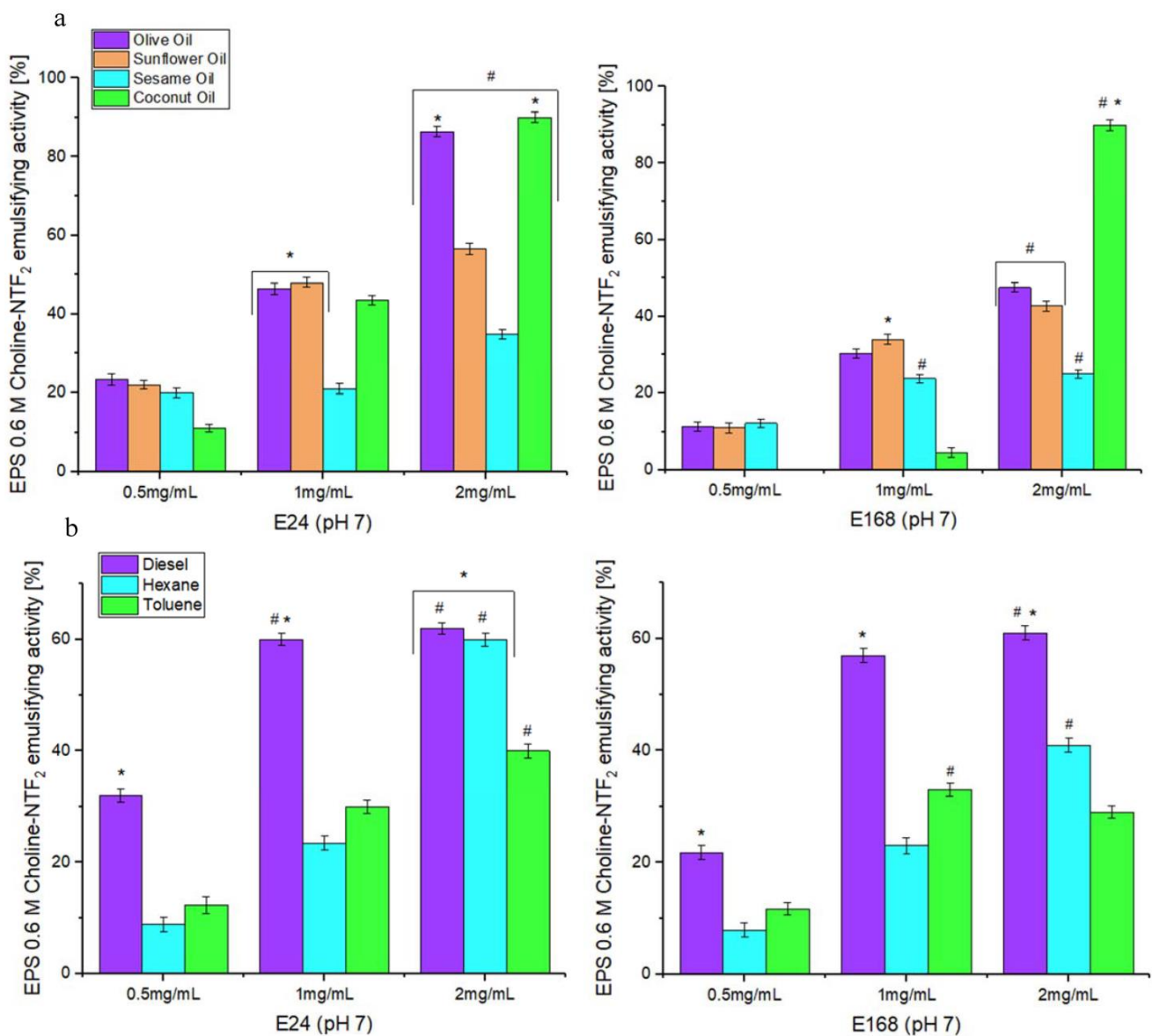


Figure 5. Emulsifying activity of EPS at different concentrations (0.5, 1, 2 mg/mL) and times (E24 y E168): (a) emulsifying activity with different natural oils, and (b) emulsifying activity with different hydrocarbons. *, statistical differences between different natural oils or hydrocarbons for each concentration ($p < 0.05$). #, statistical differences between different concentrations ($p < 0.05$).

The results indicated that EPS was very efficient at 2 mg/mL compared with the results obtained by *Pantoea* sp. [78], which required higher concentrations of EPS (5 mg/mL) to emulsify olive oil ((E24) 58.9%), sunflower oil ((E24) 52.9%), and hexane ((E24) 62%). These differences in the emulsifying capacity of the different EPSs could be due to different factors such as their chemical composition and morphology [80].

In order to see the environmental advantages of using natural polymers over commercial compounds, the EPS was also tested with three commercial emulsifiers (Triton X-100, Tween 20, and SDS), Figure 6.

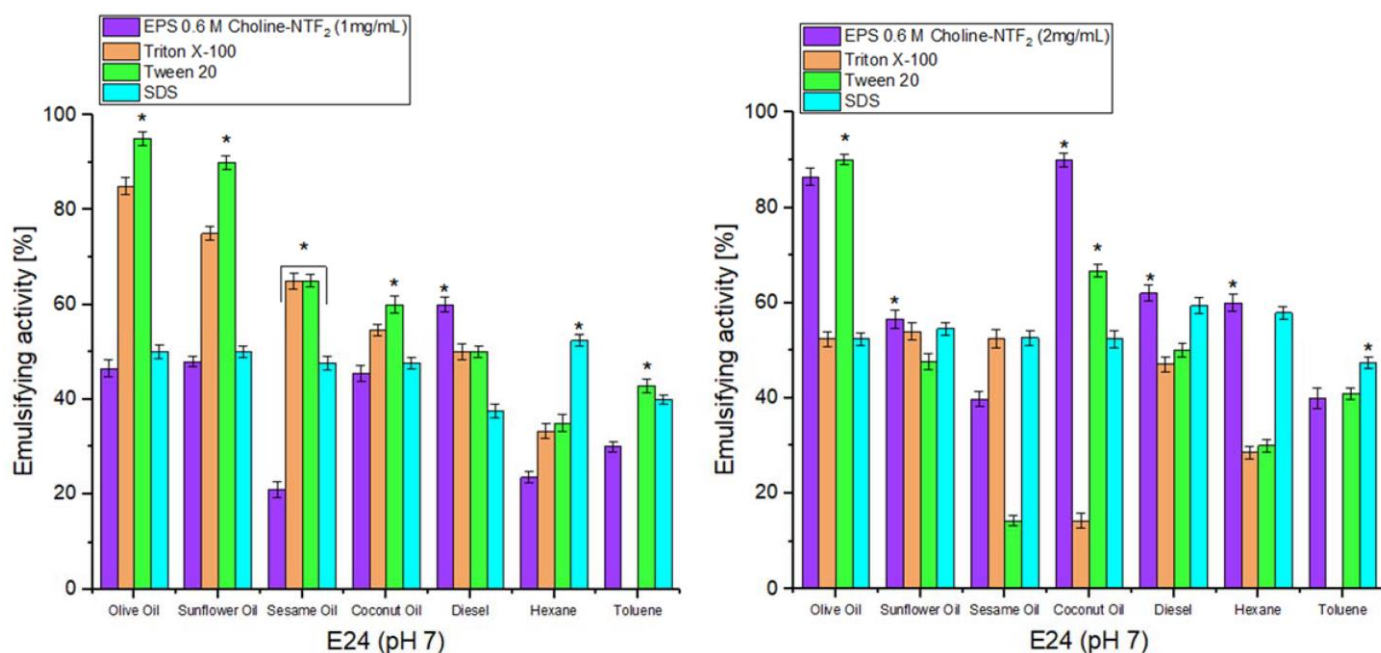


Figure 6. Comparison of emulsifying activity at different EPS 0.6 M Choline NTF₂ concentrations (1, 2 mg/mL) against commercial emulsifiers (Triton X-100, Tween 20 and SDS) across different natural oils and hydrocarbons. * ($p < 0.05$).

The results indicated that at a concentration of 1 mg, the EPS only presented a better emulsifying ($p < 0.05$) activity for diesel ((E24) 60%) compared with commercial emulsifiers (Triton X-100 ((E24) 50%), Tween 20 ((E24) 50%) and SDS ((E24) 37.5%)). However, for a concentration of 2 mg, the emulsifying activity of the EPS was significantly ($p < 0.05$) improved. This increased for olive oil ((E24) 86.4%), sunflower ((E24) 56.5%), coconut ((E24) 90%), diesel ((E24) 62%), and hexane (E24) 60%), compared with commercial emulsifiers. For the latter, only Tween 20 obtained a very slight improvement for olive oil ((E24) 90%), only 4% more when compared with EPS.

Natural EPSs have the advantage of not presenting unwanted side-effects which can be present in commercial emulsifiers [81–83]. They are more respectful to the environment for any industrial application.

The emulsifying activity study was also carried out with the other EPSs produced from biodegrading different concentrations of Choline NTF₂ (0.2 and 1.0 Choline NTF₂), at a concentration of 1 mg. This is shown in Figure 7, where the EPSs produced from 0.2, 0.6, and 1.0 M Choline NTF₂ are compared. The results indicated that for the vegetable oils and hydrocarbons, the EPSs of 0.2 M, and 1.0 M Choline NTF₂ did not have a notable emulsifying activity, with values that did not reach 20% in most cases. However, the EPS obtained from 0.6 M Choline NTF₂, presented 47% higher activity than the other EPSs for vegetable oils, and even higher in hydrocarbons, with a 60% increase in emulsifying activity for 0.6 M Choline NTF₂. This indicated that the morphology of the EPS had a decisive role in this activity [37].

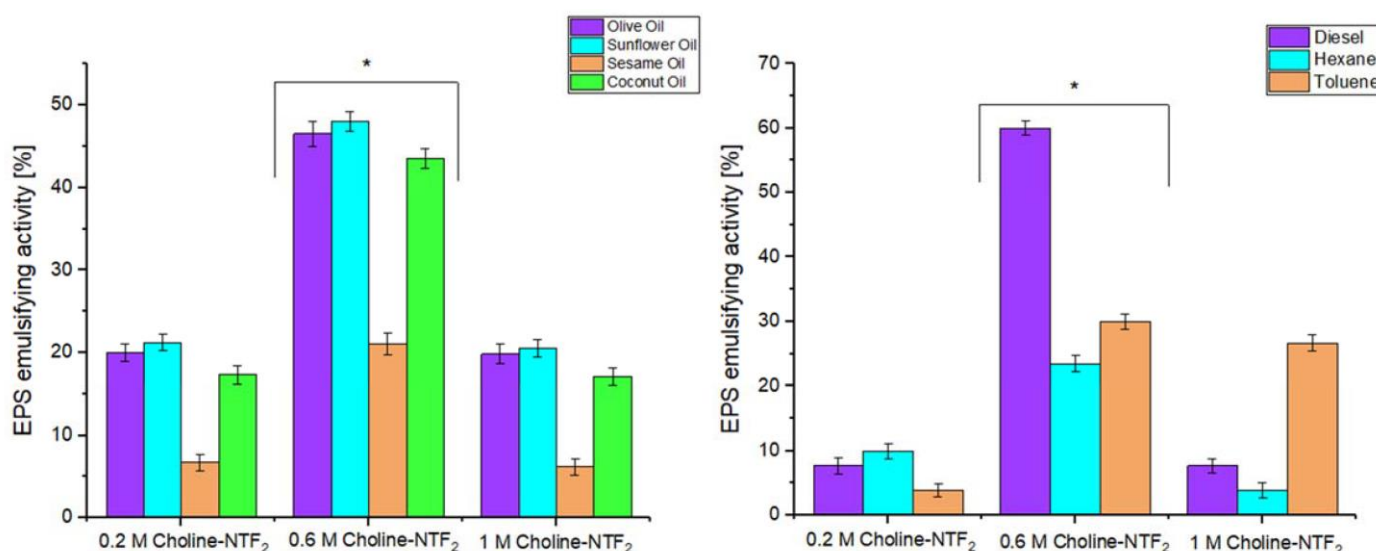


Figure 7. EPSs emulsifying activity of 0.2 M Choline NTF₂, 0.6 M Choline NTF₂ and 1.0 M Choline NTF₂ with different natural oils and hydrocarbons. * ($p < 0.05$).

3.5.2. Nonenzymatic Antioxidant, Toxicity, Non-Radical H₂O₂, Morphological Cell and Catalase (CAT) Assay

Nonenzymatic antioxidant assays as shown in Figure 8a (radical scavenging activity (DPPH), hydroxyl radical (HO•), and superoxide scavenging activities (O₂⁻)) have been used as instruments to explore the antioxidant activity of exopolysaccharides [84].

The antioxidant capacity of the EPS obtained from 0.6 M Choline NTF₂ was tested in the range of 0.1 to 10 mg/mL, for all assays. For radical scavenging activity DPPH, Figure 8a, EPS presented a high scavenging activity of $85 \pm 1.3\%$ versus $87.4 \pm 1.4\%$ of VC at 10 mg/mL. In the case of the radical scavenging activity for the hydroxyl radical (HO•), of the EPS (Figure 8a), the results indicated that the EPS had an excellent capacity, with $99 \pm 1.3\%$, thus, obtaining the same capacity as the control, named VC ($99.5 \pm 1.3\%$), at 7.5 mg/mL. For superoxide scavenging activities (O₂⁻), shown in Figure 8a, EPS had a scavenging capability of $94.3 \pm 1.3\%$ compared with VC with a scavenging capability of 100% at a concentration of only 0.1 mg/mL. The EPS presented an efficient scavenging activity compared with other EPSs obtained by different species such as *Tetragenococcus halophilus* SNTH-8 with DPPH and hydroxyl radicals activity of 63.53% and 50.19%, respectively, at 12 mg/mL [85]. *Rhodococcus qingshengii* QDR4-2 resulted in DPPH, hydroxyl and superoxide radicals of $49.09 \pm 1.54\%$, $30.24 \pm 2.82\%$, and $39.18 \pm 2.70\%$, respectively, at 3 mg/mL [86]. These results indicated that EPS was very efficient for nonenzymatic antioxidants under these environmental conditions.

The cytotoxicity results showed that EPS (0.6 M Choline NTF₂ medium), with all the tested concentrations, maintained cell viability, above 90% and very close to control Figure 8b. The results were not significantly different ($p < 0.05$). EPS did not cause damage to the tested cell line. Studies carried out in this same genus revealed that for the EPS of *Pantoea* sp. YU16-S3 [71], proliferation increased at a concentration greater than 100 µg/mL in the NIH3T3 cell line tested. This absence of cytotoxicity, in 0.6 M Choline NTF₂, in a wide range of concentrations, gives EPS a great advantage for environmental and public health applications.

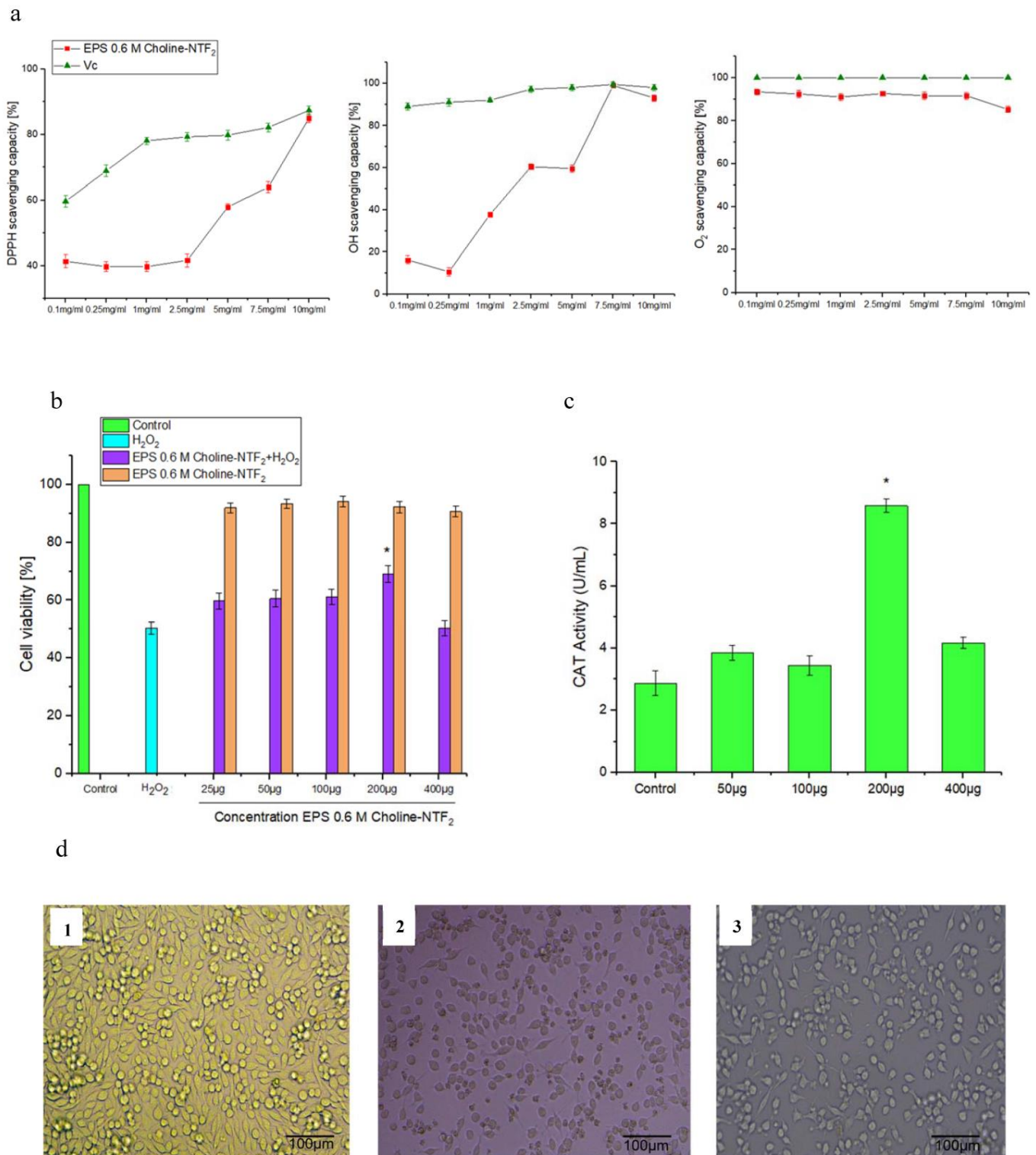


Figure 8. (a) Antioxidant effect of EPS 0.6 M Choline NTF₂ with DPPH, hydroxyl (OH) and superoxide radical. (b) Biocompatibility of EPS 0.6 M Choline NTF₂ and evaluation of the H₂O₂-damaged HeLa cells protection. (c) Catalase activity by the presence of EPS 0.6 M Choline NTF₂. (d) Effects of EPS 0.6 M Choline NTF₂ on morphological alterations of H₂O₂-damaged HeLa cells. Control was untreated HeLa cells, (1), incubated with H₂O₂ (2 mM) (2), pretreated with of EPS 0.6 M Choline NTF₂ (200 µg/mL) (3). Cells were photographed under phase contrast microscopy bar 30 µm. * ($p < 0.05$).

Cell viability and morphological study was carried out to evaluate the possible effect of a non-radical H_2O_2 . HeLa cells were highly sensitive to H_2O_2 injury, Figure 8b. A marked decrease in cell viability was shown when cells were exposed to 2 mM H_2O_2 . This meant a reduction in viability of 50.3%, Figure 8b. In addition to this, the morphology of the cells was affected at this concentration (Figure 8b). H_2O_2 interfered with the development of filipodia, unlike control cells, where these were well developed. These results indicated that an accumulation of reactive oxygen species (ROS) had occurred [38].

On the other hand, cells previously incubated with EPS exhibited a morphology typical of control cells, with good development of filipodia, Figure 8(c1), at a concentration of 200 $\mu\text{g}/\text{mL}$. Treatment with EPS at that concentration, Figure 8(c3), was found to protect against H_2O_2 -induced damage with a viability of more than 70%. This could be directly related to the morphology of the EPS (Figure 2), where it could achieve a critical scaffold structure, and this could be necessary to induce protection [34]. The reducing power of the EPS was due to its remarkable radical scavenging capacity and endowed it with potent antioxidant activity. In addition to this, an enzymatic antioxidant assay was conducted to determine the catalase (CAT), Figure 8d. EPS increased CAT activity in HeLa cells, at all concentrations tested. However, the highest CAT activity was $8.54 \pm 2.9 \text{ U}/\text{mL}$ in the presence of EPS, at a concentration of 200 $\mu\text{g}/\text{mL}$, compared with the value of $2.56 \pm 2.1 \text{ U}/\text{mL}$ of the control ($p < 0.05$). The increase in the CAT activity by the EPS allowed the prevention of the formation of hydroxyl radicals and stimulated the enzymatic defence of the cells [87]. The ability of other EPSs to protect against this cell damage has been described in *Lactobacillus kimchi* SR8 ($8.78 \pm 0.31 \text{ U}/\text{mL}$ at 50 mg/Kg) [88] and in other genera such as *Lactococcus lactis* ($8.19 \pm 1.36 \text{ U}/\text{mL}$ at 40 mg/Kg) [89]. This reveals that EPS can effectively act as an antioxidant preventing lipid peroxidation of the membrane.

3.5.3. Chelating Activity and Antibacterial Activity

EPS obtained from the biodegradation of 0.6 M Choline NTF_2 presented an iron chelation (Figure 9a,b) capacity of 42.2% and 52.4% at 2.5 and 5 mg/mL, respectively, for pH 5.6. These results demonstrated that EPS was better than the EPSs previously isolated from *Bacillus amyloliquefaciens*, as it exhibited a chelating capacity on Fe^{2+} at 2 mg/mL of up to 30.5% [90]. The chelating capacity of the polymer contributed to preventing the formation of free radicals. This was due to the presence in the exopolysaccharide of specific functional groups (OH and COO^-) [91]. Furthermore, under limiting environmental conditions, the EPS appears as a good candidate in bioremediation processes.

On the other hand, the results of the antimicrobial activity of EPS showed a strong zone of inhibition with a halo over 15 mm where the bacterial growth was inhibited for one of the tested strains. EPS was able to prevent the growth of *Staphylococcus aureus* CECT 8753 ($15.0 \pm 0.4 \text{ mm}$), Figure 9c,d, at the highest concentration tested. Different studies demonstrate the antimicrobial capacity of EPSs from marine bacteria with the capacity to inhibit bacterial pathogens [92]. This antimicrobial activity could be directly related to the chelation capacity of EPS. This could hinder the absorption of nutrients and vital processes of synthesis of genetic material [43,93].

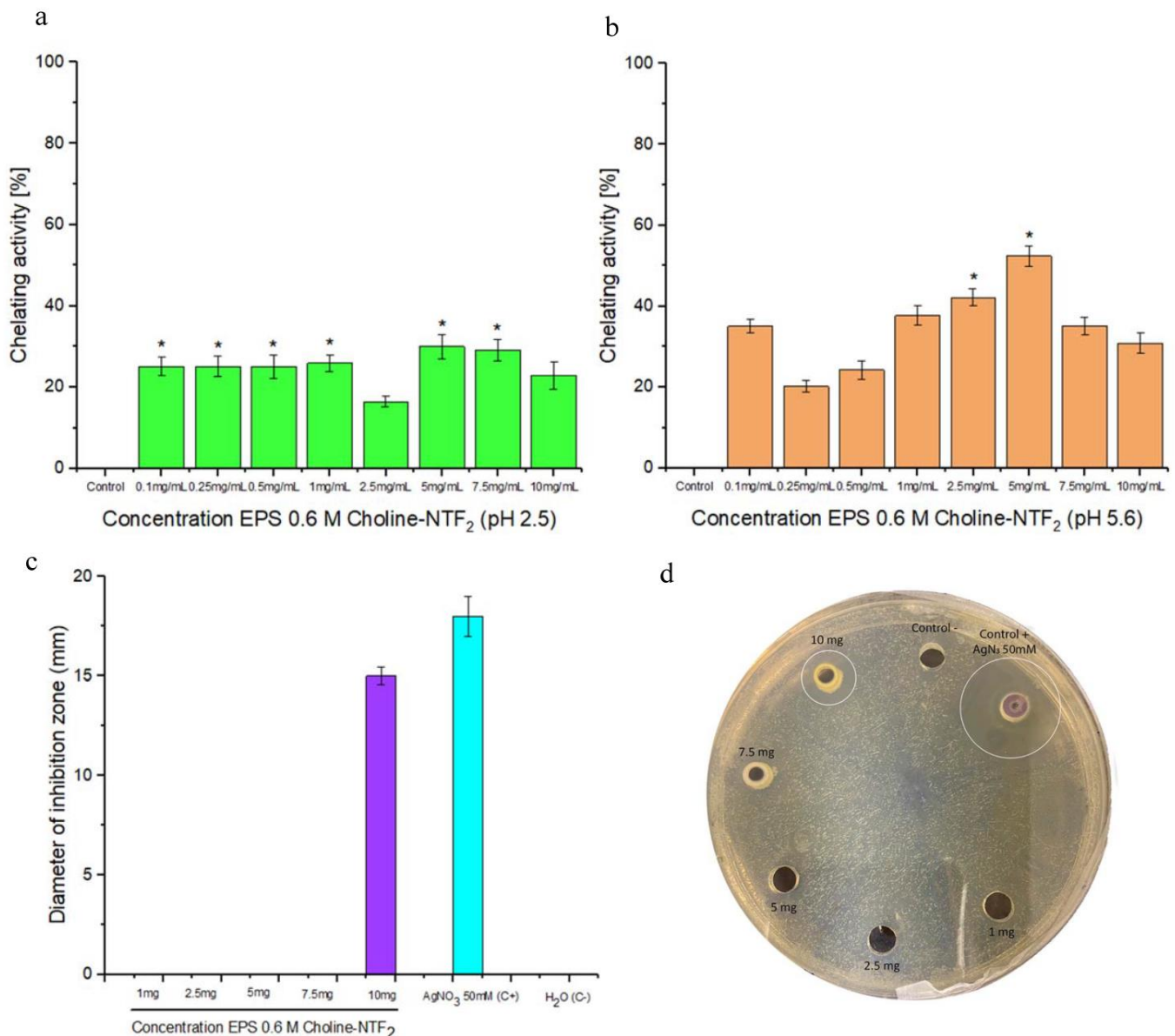


Figure 9. Chelating activity at different concentrations of EPS 0.6 M Choline NTF₂ measured at pH (a) 5.6 and (b) 2.5. (c) Diameter of inhibition zone of EPS 0.6 M Choline NTF₂ on *Staphylococcus aureus*. (d) Image of the inhibition halo of EPS 0.6 M Choline NTF₂. * $p < 0.05$.

4. Conclusions

Pantoea. agglomerans uam8 isolated from ionic liquid Choline NTF₂ is presented as a good candidate for its biodegradation under saline stress conditions. This study provides valuable information on the behavior of the exopolysaccharides produced from the biodegradation of an ionic liquid. Varying the osmolarity conditions of the medium had an effect on the morphology of the produced exopolysaccharides whilst the chemical composition remained unchanged. The exopolysaccharide produced in 0.6 M conditions had the highest emulsifying activity for natural oils and hydrocarbons compared with those produced in different osmolarities. The 0.6 M Choline NTF₂ exopolysaccharide did not present cytotoxicity and had antioxidant capabilities. Furthermore, this EPS had other important biotechnological advantages, such as chelating and antimicrobial properties. The role of these polymers produced by bacteria in biodegradation processes opens up an important avenue of research, to glimpse how they can influence the environment where they are produced, and their direct relationship with the environment.

Author Contributions: Conceptualization, formal analysis, investigation, data curation, funding acquisition, methodology, validation, resources, supervision, writing—original draft, writing—review and editing, A.C.; funding acquisition, project administration, manuscript review, A.R.; formal analysis, investigation, writing—original draft, S.-L.E. All authors have read and agreed to the published version of the manuscript.

Funding: This research was funded by the Spanish Ministry of Science and Innovation for financial support (project PID2022-136607NB-I00) and FUAM, Universidad Autónoma de Madrid, Spain (project number 820053).

Institutional Review Board Statement: Not applicable.

Informed Consent Statement: Not applicable.

Data Availability Statement: Not available.

Conflicts of Interest: The authors declare no conflict of interest.

References

1. Akoh, C.C.; Chang, S.W.; Lee, G.C.; Shaw, J.F. Biocatalysis for the Production of Industrial Products and Functional Foods from Rice and Other Agricultural Produce. *J. Agric. Food Chem.* **2008**, *56*, 10445–10451. [[CrossRef](#)] [[PubMed](#)]
2. Singh, S.K.; Savoy, A.W. Ionic Liquids Synthesis and Applications: An Overview. *J. Mol. Liq.* **2020**, *297*, 112038. [[CrossRef](#)]
3. Barciela, P.; Perez-Vazquez, A.; Prieto, M.A. Azo Dyes in the Food Industry: Features, Classification, Toxicity, Alternatives, and Regulation. *Food Chem. Toxicol.* **2023**, *178*, 113935. [[CrossRef](#)] [[PubMed](#)]
4. Daughton, C.G.; Ruhoy, I.S. Green Pharmacy and PharmEcovigilance: Prescribing and the Planet. *Expert Rev. Clin. Pharmacol.* **2011**, *4*, 211–232. [[CrossRef](#)] [[PubMed](#)]
5. Thomaidis, N.S.; Asimakopoulos, A.G.; Bletsou, A.A. Emerging Contaminants: A Tutorial Mini-Review. *Glob. NEST J.* **2012**, *14*, 72–79. [[CrossRef](#)]
6. Rudnicka-Kepa, P.; Beldowska, M.; Zaborska, A. Enhanced Heavy Metal Discharges to Marine Deposits in Glacial Bays of Two Arctic Fjords (Hornsund and Kongsfjorden). *J. Mar. Syst.* **2024**, *241*, 103915. [[CrossRef](#)]
7. Li, S.; Wang, H.; He, Y.; Liang, D.; Shen, Y.; Gu, Q.; Zeng, Y. How Microplastic Loads Relate to Natural Conditions and Anthropogenic Activities in the Yangtze River Basin. *Chemosphere* **2023**, *342*, 140146. [[CrossRef](#)]
8. Marimuthu, T.; Sidat, Z.; Kumar, P.; Choonara, Y.E. An Imidazolium-Based Ionic Liquid as a Model to Study Plasticization Effects on Cationic Polymethacrylate Films. *Polymers* **2023**, *15*, 1239. [[CrossRef](#)]
9. Cho, C.W.; Pham, T.P.T.; Zhao, Y.; Stolte, S.; Yun, Y.S. Review of the Toxic Effects of Ionic Liquids. *Sci. Total Environ.* **2021**, *786*, 147309. [[CrossRef](#)]
10. Abdelghany, T.M.; Leitch, A.C.; Nevjestić, I.; Ibrahim, I.; Miwa, S.; Wilson, C.; Heutz, S.; Wright, M.C. Emerging Risk from “Environmentally-Friendly” Solvents: Interaction of Methylimidazolium Ionic Liquids with the Mitochondrial Electron Transport Chain Is a Key Initiation Event in Their Mammalian Toxicity. *Food Chem. Toxicol.* **2020**, *145*, 111593. [[CrossRef](#)]
11. Tan, Z.Q.; Liu, J.F.; Pang, L. Advances in Analytical Chemistry Using the Unique Properties of Ionic Liquids. *TrAC—Trends Anal. Chem.* **2012**, *39*, 218–227. [[CrossRef](#)]
12. Ma, J.; Zhou, S.; Lai, Y.; Wang, Z.; Ni, N.; Dai, F.; Xu, Y.; Yang, X. Ionic Liquids Facilitate the Dispersion of Branched Polyethyleneimine Grafted ZIF-8 for Reinforced Epoxy Composites. *Polymers* **2023**, *15*, 1837. [[CrossRef](#)] [[PubMed](#)]
13. Greer, A.J.; Jacquemin, J.; Hardacre, C. Industrial Applications of Ionic Liquids. *Molecules* **2020**, *25*, 5207. [[CrossRef](#)] [[PubMed](#)]
14. Cvjetko Bubalo, M.; Radošević, K.; Radojčić Redovniković, I.; Halambek, J.; Gaurina Srček, V. A Brief Overview of the Potential Environmental Hazards of Ionic Liquids. *Ecotoxicol. Environ. Saf.* **2014**, *99*, 1–12. [[CrossRef](#)]
15. Matzke, M.; Thiele, K.; Müller, A.; Filser, J. Sorption and Desorption of Imidazolium Based Ionic Liquids in Different Soil Types. *Chemosphere* **2009**, *74*, 568–574. [[CrossRef](#)] [[PubMed](#)]
16. Gonzalez-Miquel, M.; Bedia, J.; Abrusci, C.; Palomar, J.; Rodriguez, F. Anion Effects on Kinetics and Thermodynamics of CO₂ Absorption in Ionic Liquids. *J. Phys. Chem. B* **2013**, *117*, 3398–3406. [[CrossRef](#)]
17. Palomar, J.; Gonzalez-Miquel, M.; Polo, A.; Rodriguez, F. Understanding the Physical Absorption of CO₂ in Ionic Liquids Using the COSMO-RS Method. *Ind. Eng. Chem. Res.* **2011**, *50*, 3452–3463. [[CrossRef](#)]
18. An, Y.X.; Zong, M.H.; Wu, H.; Li, N. Pretreatment of Lignocellulosic Biomass with Renewable Cholinium Ionic Liquids: Biomass Fractionation, Enzymatic Digestion and Ionic Liquid Reuse. *Bioresour. Technol.* **2015**, *192*, 165–171. [[CrossRef](#)]
19. Zhang, Q.; De Oliveira Vigier, K.; Royer, S.; Jérôme, F. Deep Eutectic Solvents: Syntheses, Properties and Applications. *Chem. Soc. Rev.* **2012**, *41*, 7108–7146. [[CrossRef](#)]
20. Lu, J.; Yan, F.; Texter, J. Advanced Applications of Ionic Liquids in Polymer Science. *Prog. Polym. Sci.* **2009**, *34*, 431–448. [[CrossRef](#)]
21. Costa, S.P.F.; Azevedo, A.M.O.; Pinto, P.C.A.G.; Saraiva, M.L.M.F.S. Environmental Impact of Ionic Liquids: Recent Advances in (Eco)Toxicology and (Bio)Degradability. *ChemSusChem* **2017**, *10*, 2321–2347. [[CrossRef](#)] [[PubMed](#)]
22. Zhang, Y.; Ji, X.; Lu, X. *Choline-Based Deep Eutectic Solvents for Mitigating Carbon Dioxide Emissions*; Elsevier B.V.: Amsterdam, The Netherlands, 2015; ISBN 9780444632593.

23. Abrusci, C.; Palomar, J.; Pablos, J.L.; Rodriguez, F.; Catalina, F. Efficient Biodegradation of Common Ionic Liquids by *Sphingomonas paucimobilis* Bacterium. *Green. Chem.* **2011**, *13*, 709–717. [[CrossRef](#)]
24. Jordan, A.; Gathergood, N. Biodegradation of Ionic Liquids—a Critical Review. *Chem. Soc. Rev.* **2015**, *44*, 8200–8237. [[CrossRef](#)] [[PubMed](#)]
25. Hou, X.D.; Liu, Q.P.; Smith, T.J.; Li, N.; Zong, M.H. Evaluation of Toxicity and Biodegradability of Cholinium Amino Acids Ionic Liquids. *PLoS ONE* **2013**, *8*, e59145. [[CrossRef](#)]
26. Liu, Y.; Li, J. Role of *Pseudomonas aeruginosa* Biofilm in the Initial Adhesion, Growth and Detachment of *Escherichia coli* in Porous Media. *Environ. Sci. Technol.* **2008**, *42*, 443–449. [[CrossRef](#)]
27. Kaur, N.; Dey, P. Bacterial Exopolysaccharides as Emerging Bioactive Macromolecules: From Fundamentals to Applications. *Res. Microbiol.* **2023**, *174*, 104024. [[CrossRef](#)] [[PubMed](#)]
28. Dedhia, N.; Marathe, S.J.; Singhal, R.S. Food Polysaccharides: A Review on Emerging Microbial Sources, Bioactivities, Nanoformulations and Safety Considerations. *Carbohydr. Polym.* **2022**, *287*, 119355. [[CrossRef](#)]
29. Abrusci, C.; Pablos, J.L.; Corrales, T.; López-Marín, J.; Marín, I.; Catalina, F. Biodegradation of Photo-Degraded Mulching Films Based on Polyethylenes and Stearates of Calcium and Iron as pro-Oxidant Additives. *Int. Biodeterior. Biodegrad.* **2011**, *65*, 451–459. [[CrossRef](#)]
30. Abrusci, C.; Martín-González, A.; Del Amo, A.; Corrales, T.; Catalina, F. Biodegradation of Type-B Gelatine by Bacteria Isolated from Cinematographic Films. A Viscometric Study. *Polym. Degrad. Stab.* **2004**, *86*, 283–291. [[CrossRef](#)]
31. Morro, A.; Catalina, F.; Corrales, T.; Pablos, J.L.; Marin, I.; Abrusci, C. New Blends of Ethylene-Butyl Acrylate Copolymers with Thermoplastic Starch. Characterization and Bacterial Biodegradation. *Carbohydr. Polym.* **2016**, *149*, 68–76. [[CrossRef](#)]
32. Thompson, J.D.; Gibson, T.J.; Plewniak, F.; Jeanmougin, F.; Higgins, D.G. The CLUSTAL X Windows Interface: Flexible Strategies for Multiple Sequence Alignment Aided by Quality Analysis Tools. *Nucleic Acids Res.* **1997**, *25*, 4876–4882. [[CrossRef](#)] [[PubMed](#)]
33. Abrusci, C.; Marquina, D.; Del Amo, A.; Catalina, F. Biodegradation of Cinematographic Gelatin Emulsion by Bacteria and Filamentous Fungi Using Indirect Impedance Technique. *Int. Biodeterior. Biodegrad.* **2007**, *60*, 137–143. [[CrossRef](#)]
34. Sánchez-León, E.; Bello-Morales, R.; López-Guerrero, J.A.; Poveda, A.; Jiménez-Barbero, J.; Gironès, N.; Abrusci, C. Isolation and Characterization of an Exopolymer Produced by *Bacillus licheniformis*: In Vitro Antiviral Activity against Enveloped Viruses. *Carbohydr. Polym.* **2020**, *248*, 116737. [[CrossRef](#)] [[PubMed](#)]
35. Sedlacek, P.; Slaninova, E.; Koller, M.; Nebesarova, J.; Marova, I.; Krzyzaneck, V.; Obruca, S. PHA Granules Help Bacterial Cells to Preserve Cell Integrity When Exposed to Sudden Osmotic Imbalances. *N. Biotechnol.* **2019**, *49*, 129–136. [[CrossRef](#)] [[PubMed](#)]
36. Morro, A.; Catalina, F.; Pablos, J.L.; Corrales, T.; Marin, I.; Abrusci, C. Surface Modification of Poly(ϵ -Caprolactone) by Oxygen Plasma for Antibacterial Applications. Biocompatibility and Monitoring of Live Cells. *Eur. Polym. J.* **2017**, *94*, 405–416. [[CrossRef](#)]
37. Sánchez-león, E.; Huang-lin, E.; Amils, R.; Abrusci, C. Production and Characterisation of an Exopolysaccharide by *Bacillus amyloliquefaciens*: Biotechnological Applications. *Polymers* **2023**, *15*, 1550. [[CrossRef](#)]
38. Huang-Lin, E.; Sánchez-León, E.; Amils, R.; Abrusci, C. Potential Applications of an Exopolysaccharide Produced by *Bacillus xiamenensis* RT6 Isolated from an Acidic Environment. *Polymers* **2022**, *14*, 3918. [[CrossRef](#)]
39. Morro, A.; Catalina, F.; Sanchez-León, E.; Abrusci, C. Photodegradation and Biodegradation Under Thermophile Conditions of Mulching Films Based on Poly(Butylene Adipate-Co-Terephthalate) and Its Blend with Poly(Lactic Acid). *J. Polym. Environ.* **2019**, *27*, 352–363. [[CrossRef](#)]
40. Cooper, D.G.; Goldenberg, B.G. Surface-Active Agents from Two *Bacillus* Species. *Appl. Environ. Microbiol.* **1987**, *53*, 224–229. [[CrossRef](#)]
41. Pérez-Blanco, C.; Huang-Lin, E.; Abrusci, C. Characterization, Biodegradation and Cytotoxicity of Thermoplastic Starch and Ethylene-Vinyl Alcohol Copolymer Blends. *Carbohydr. Polym.* **2022**, *298*, 120085. [[CrossRef](#)]
42. Liu, Z.; Dong, L.; Jia, K.; Zhan, H.; Zhang, Z.; Shah, N.P.; Tao, X.; Wei, H. Sulfonation of *Lactobacillus plantarum* WLPL04 Exopolysaccharide Amplifies Its Antioxidant Activities in Vitro and in a Caco-2 Cell Model. *J. Dairy Sci.* **2019**, *102*, 5922–5932. [[CrossRef](#)] [[PubMed](#)]
43. Rajoka, M.S.R.; Mehwish, H.M.; Hayat, H.F.; Hussain, N.; Sarwar, S.; Aslam, H.; Nadeem, A.; Shi, J. Characterization, the Antioxidant and Antimicrobial Activity of Exopolysaccharide Isolated from Poultry Origin *Lactobacilli*. *Probiotics Antimicrob. Proteins* **2019**, *11*, 1143–1144. [[CrossRef](#)] [[PubMed](#)]
44. Morin, A.; Parveen, Z. *Pantoea*. *Encycl. Food Microbiol.* **1999**, *3*, 1623–1630.
45. Delétoile, A.; Décré, D.; Courant, S.; Passet, V.; Audo, J.; Grimont, P.; Arlet, G.; Brisse, S. Phylogeny and Identification of *Pantoea* Species and Typing of *Pantoea agglomerans* Strains by Multilocus Gene Sequencing. *J. Clin. Microbiol.* **2009**, *47*, 300–310. [[CrossRef](#)] [[PubMed](#)]
46. Loch, T.P.; Faisal, M. Isolation of *Pantoea agglomerans* from Brown Trout (*Salmo Trutta*) from Gilchrist Creek, Michigan, USA. *Bull. Eur. Assoc. Fish Pathol.* **2007**, *27*, 200–204.
47. Raad, Z.; Hassan, S.; Mohammed, A. Temperature Effects on Growth of the Biocontrol Agent *Pantoea agglomerans* (An Oval Isolate from Iraqi Soils). *J. Adv. Lab. Res. Biol.* **2017**, *8*, 85–88.
48. Brady, C.L.; Venter, S.N.; Cleenwerck, I.; Engelbeen, K.; Vancanneyt, M.; Swings, J.; Coutinho, T.A. *Pantoea vagans* sp. Nov., *Pantoea eucalypti* sp. Nov., *Pantoea deleyi* sp. Nov. and *Pantoea anthophila* sp. Nov. *Int. J. Syst. Evol. Microbiol.* **2009**, *59*, 2339–2345. [[CrossRef](#)]

49. Popp, A.; Cleenwerck, I.; Iversen, C.; De Vos, P.; Stephan, R. *Pantoea gaviniae* sp. Nov. and *Pantoea calida* sp. Nov., Isolated from Infant Formula and an Infant Formula Production Environment. *Int. J. Syst. Evol. Microbiol.* **2010**, *60*, 2786–2792. [[CrossRef](#)]
50. Suleimanova, A.D.; Itkina, D.L.; Pudova, D.S.; Sharipova, M.R. Identification of *Pantoea* Phytate-Hydrolyzing Rhizobacteria Based on Their Phenotypic Features and Multilocus Sequence Analysis (MLSA). *Microbiology* **2021**, *90*, 87–95. [[CrossRef](#)]
51. Silvi, S.; Barghini, P.; Aquilanti, A.; Juarez-Jimenez, B.; Fenice, M. Physiologic and Metabolic Characterization of a New Marine Isolate (BM39) of *Pantoea* sp. Producing High Levels of Exopolysaccharide. *Microb. Cell Fact.* **2013**, *12*, 10. [[CrossRef](#)]
52. Quesada, E.; Bejar, V.; Calvo, C. Exopolysaccharide Production by *Volcaniella eurihalina*. *Experientia* **1993**, *49*, 1037–1041. [[CrossRef](#)]
53. Gu, D.; Jiao, Y.; Wu, J.; Liu, Z.; Chen, Q. Optimization of EPS Production and Characterization by a Halophilic Bacterium, *Kocuria rosea* ZJUQH from Chaka Salt Lake with Response Surface Methodology. *Molecules* **2017**, *22*, 814. [[CrossRef](#)] [[PubMed](#)]
54. Seesuriyachan, P.; Kuntiya, A.; Hanmoungjai, P.; Techapun, C.; Chaiyaso, T.; Leksawasdi, N. Optimization of Exopolysaccharide Overproduction by *Lactobacillus confusus* in Solid State Fermentation under High Salinity Stress. *Biosci. Biotechnol. Biochem.* **2012**, *76*, 912–917. [[CrossRef](#)] [[PubMed](#)]
55. Poli, A.; Anzelmo, G.; Nicolaus, B. Bacterial Exopolysaccharides from Extreme Marine Habitats: Production, Characterization and Biological Activities. *Mar. Drugs* **2010**, *8*, 1779–1802. [[CrossRef](#)]
56. Firth, E.; Carpenter, S.D.; Sørensen, H.L.; Collins, R.E.; Deming, J.W. Bacterial Use of Choline to Tolerate Salinity Shifts in Sea-Ice Brines. *Elementa* **2016**, *2016*, 000120. [[CrossRef](#)]
57. Kaplan, C.P.; Porter, R.K.; Brand, M.D. The Choline Transporter Is the Major Site of Control of Choline Oxidation in Isolated Rat Liver Mitochondria. *FEBS Lett.* **1993**, *321*, 24–26. [[CrossRef](#)] [[PubMed](#)]
58. Landfald, B.; Strom, A.R. Choline-Glycine Betaine Pathway Confers a High Level of Osmotic Tolerance in *Escherichia coli*. *J. Bacteriol.* **1986**, *165*, 849–855. [[CrossRef](#)] [[PubMed](#)]
59. Sand, M.; Stahl, J.; Waclawska, I.; Ziegler, C.; Averhoff, B. Identification of an Osmo-Dependent and an Osmo-Independent Choline Transporter in *Acinetobacter baylyi*: Implications in Osmostress Protection and Metabolic Adaptation. *Environ. Microbiol.* **2014**, *16*, 1490–1502. [[CrossRef](#)]
60. Sydow, M.; Owsianiak, M.; Framski, G.; Woźniak-Karczewska, M.; Piotrowska-Cyplik, A.; Ławniczak, Ł.; Szulc, A.; Zgoła-Grześkowiak, A.; Heipieper, H.J.; Chrzanowski, Ł. Biodiversity of Soil Bacteria Exposed to Sub-Lethal Concentrations of Phosphonium-Based Ionic Liquids: Effects of Toxicity and Biodegradation. *Ecotoxicol. Environ. Saf.* **2018**, *147*, 157–164. [[CrossRef](#)]
61. Dutkiewicz, J.; Mackiewicz, B.; Lemieszek, M.K.; Golec, M.; Milanowski, J. *Pantoea agglomerans*: A Mysterious Bacterium of Evil and Good. Part IV. Beneficial Effects. *Ann. Agric. Environ. Med.* **2016**, *23*, 206–222. [[CrossRef](#)]
62. El-Bestawy, E.; Mansy, A.H.; Attia, A.M.; Zahran, H. Biodegradation of Persistent Chlorinated Hydrocarbons Using Selected Freshwater Bacteria. *J. Bioremediation Biodegrad.* **2016**, *7*, 1–6. [[CrossRef](#)]
63. Boch, J.; Kempf, B.; Bremer, E. Osmoregulation in *Bacillus subtilis*: Synthesis of the Osmoprotectant Glycine Betaine from Exogenously Provided Choline. *J. Bacteriol.* **1994**, *176*, 5364–5371. [[CrossRef](#)] [[PubMed](#)]
64. Rath, H.; Reeder, A.; Hoffmann, T.; Hammer, E.; Seubert, A.; Bremer, E.; Völker, U.; Mäder, U. Management of Osmoprotectant Uptake Hierarchy in *Bacillus subtilis* via a SigB-Dependent Antisense RNA. *Front. Microbiol.* **2020**, *11*, 622. [[CrossRef](#)] [[PubMed](#)]
65. Robert, H.; Le Marrec, C.; Blanco, C.; Jebbar, M. Glycine Betaine, Carnitine, and Choline Enhance Salinity Tolerance and Prevent the Accumulation of Sodium to a Level Inhibiting Growth of *Tetragenococcus halophila*. *Appl. Environ. Microbiol.* **2000**, *66*, 509–517. [[CrossRef](#)] [[PubMed](#)]
66. Reardon, C.L.; Dohnalkova, A.C.; Nachimuthu, P.; Kennedy, D.W.; Saffarini, D.A.; Arey, B.W.; Shi, L.; Wang, Z.; Moore, D.; McLean, J.S.; et al. Role of Outer-Membrane Cytochromes MtrC and OmcA in the Biomineralization of Ferrihydrite by *Shewanella oneidensis* MR-1. *Geobiology* **2010**, *8*, 56–68. [[CrossRef](#)] [[PubMed](#)]
67. Solmaz, K.B.; Ozcan, Y.; Dogan, N.M.; Bozkaya, O.; Ide, S. Characterization and Production of Extracellular Polysaccharides (EPS) by *Bacillus pseudomycooides* U10. *Environments* **2018**, *5*, 63. [[CrossRef](#)]
68. de Brito, M.M.; Bundeleva, I.; Marin, F.; Vennin, E.; Wilmotte, A.; Plasseraud, L.; Visscher, P.T. Effect of Culture PH on Properties of Exopolymeric Substances from *Synechococcus* PCC7942: Implications for Carbonate Precipitation. *Geosciences* **2022**, *12*, 210. [[CrossRef](#)]
69. Li, L.; Huang, T.; Liu, H.; Zang, J.; Wang, P.; Jiang, X. Purification, Structural Characterization and Anti-UVB Irradiation Activity of an Extracellular Polysaccharide from *Pantoea agglomerans*. *Int. J. Biol. Macromol.* **2019**, *137*, 1002–1012. [[CrossRef](#)]
70. Eudes, A.; Juminaga, D.; Baidoo, E.E.K.; Collins, F.W.; Keasling, J.D.; Loqué, D. Production of Hydroxycinnamoyl Anthranilates from Glucose in *Escherichia coli*. *Microb. Cell Fact.* **2013**, *12*, 62. [[CrossRef](#)]
71. Sahana, T.G.; Rekha, P.D. A Novel Exopolysaccharide from Marine Bacterium *Pantoea* sp. YU16-S3 Accelerates Cutaneous Wound Healing through Wnt/ β -Catenin Pathway. *Carbohydr. Polym.* **2020**, *238*, 116191. [[CrossRef](#)]
72. Hong, T.; Yin, J.Y.; Nie, S.P.; Xie, M.Y. Applications of Infrared Spectroscopy in Polysaccharide Structural Analysis: Progress, Challenge and Perspective. *Food Chem. X* **2021**, *12*, 100168. [[CrossRef](#)] [[PubMed](#)]
73. Sun, H.H.; Mao, W.J.; Chen, Y.; Guo, S.D.; Li, H.Y.; Qi, X.H.; Chen, Y.L.; Xu, J. Isolation, Chemical Characteristics and Antioxidant Properties of the Polysaccharides from Marine Fungus *Penicillium* sp. F23-2. *Carbohydr. Polym.* **2009**, *78*, 117–124. [[CrossRef](#)]
74. Xiu, W.; Wang, X.; Yu, S.; Na, Z.; Li, C.; Yang, M.; Ma, Y. Structural Characterization, In Vitro Digestion Property, and Biological Activity of Sweet Corn Cob Polysaccharide Iron (III) Complexes. *Molecules* **2023**, *28*, 2961. [[CrossRef](#)] [[PubMed](#)]
75. Pirayesh, H.; Park, B.D.; Khanjanzadeh, H.; Park, H.J.; Cho, Y.J. Nanocellulose-Based Ammonia Sensitive Smart Colorimetric Hydrogels Integrated with Anthocyanins to Monitor Pork Freshness. *Food Control* **2023**, *147*, 109595. [[CrossRef](#)]

76. Shang, M.; Zhang, X.; Dong, Q.; Yao, J.; Liu, Q.; Ding, K. Isolation and Structural Characterization of the Water-Extractable Polysaccharides from *Cassia Obtusifolia* Seeds. *Carbohydr. Polym.* **2012**, *90*, 827–832. [[CrossRef](#)] [[PubMed](#)]
77. Sun, L.; Yang, Y.; Lei, P.; Li, S.; Xu, H.; Wang, R.; Qiu, Y.; Zhang, W. Structure Characterization, Antioxidant and Emulsifying Capacities of Exopolysaccharide Derived from *Pantoea alhagi* NX-11. *Carbohydr. Polym.* **2021**, *261*, 117872. [[CrossRef](#)] [[PubMed](#)]
78. Niknezhad, S.V.; Najafpour-Darzi, G.; Morowvat, M.H.; Ghasemi, Y. Exopolysaccharide Production of *Pantoea* sp. BCCS 001 GH: Physical Characterizations, Emulsification, and Antioxidant Activities. *Int. J. Biol. Macromol.* **2018**, *118*, 1103–1111. [[CrossRef](#)]
79. Niknezhad, S.V.; Kianpour, S.; Jafarzadeh, S.; Alishahi, M.; Najafpour Darzi, G.; Morowvat, M.H.; Ghasemi, Y.; Shavandi, A. Biosynthesis of Exopolysaccharide from Waste Molasses Using *Pantoea* sp. BCCS 001 GH: A Kinetic and Optimization Study. *Sci. Rep.* **2022**, *12*, 10128. [[CrossRef](#)]
80. Maalej, H.; Hmidet, N.; Boisset, C.; Bayma, E.; Heyraud, A.; Nasri, M. Rheological and Emulsifying Properties of a Gel-like Exopolysaccharide Produced by *Pseudomonas stutzeri* AS22. *Food Hydrocoll.* **2016**, *52*, 634–647. [[CrossRef](#)]
81. Furuhashi, H.; Higashiyama, M.; Okada, Y.; Kurihara, C.; Wada, A.; Horiuchi, K.; Hanawa, Y.; Mizoguchi, A.; Nishii, S.; Inaba, K.; et al. Dietary Emulsifier Polysorbate-80-Induced Small-Intestinal Vulnerability to Indomethacin-Induced Lesions via Dysbiosis. *J. Gastroenterol. Hepatol.* **2020**, *35*, 110–117. [[CrossRef](#)]
82. Banat, I.M.; Makkar, R.S.; Cameotra, S.S. Potential Commercial Applications of Microbial Surfactants. *Appl. Microbiol. Biotechnol.* **2000**, *53*, 495–508. [[CrossRef](#)] [[PubMed](#)]
83. Huang, K.H.; Chen, B.Y.; Shen, F.T.; Young, C.C. Optimization of Exopolysaccharide Production and Diesel Oil Emulsifying Properties in Root Nodulating Bacteria. *World J. Microbiol. Biotechnol.* **2012**, *28*, 1367–1373. [[CrossRef](#)] [[PubMed](#)]
84. Li, S.; Huang, R.; Shah, N.P.; Tao, X.; Xiong, Y.; Wei, H. Antioxidant and Antibacterial Activities of Exopolysaccharides from *Bifidobacterium bifidum* WBIN03 and *Lactobacillus plantarum* R315. *J. Dairy Sci.* **2014**, *97*, 7334–7343. [[CrossRef](#)] [[PubMed](#)]
85. Yang, X.; Wu, J.R.; An, F.; Xu, J.; Munchdrigel, Wei, L.; Li, M.; Bilige, M.; Wu, R. Structure Characterization, Antioxidant and Emulsifying Capacities of Exopolysaccharide Derived from *Tetragenococcus halophilus* SNTH-8. *Int. J. Biol. Macromol.* **2022**, *208*, 288–298. [[CrossRef](#)] [[PubMed](#)]
86. Li, F.; Hu, X.; Li, J.; Sun, X.; Luo, C.; Zhang, X.; Li, H.; Lu, J.; Li, Y.; Bao, M. Purification, Structural Characterization, Antioxidant and Emulsifying Capabilities of Exopolysaccharide Produced by *Rhodococcus qingshengii* QDR4-2. *J. Polym. Environ.* **2023**, *31*, 64–80. [[CrossRef](#)]
87. Govindan, S.; Johnson, E.E.R.; Christopher, J.; Shanmugam, J.; Thirumalairaj, V.; Gopalan, J. Antioxidant and Anti-Aging Activities of Polysaccharides from *Calocybe indica* Var. APK2. *Exp. Toxicol. Pathol.* **2016**, *68*, 329–334. [[CrossRef](#)] [[PubMed](#)]
88. Zhang, Y.; Chen, X.; Hu, P.; Liao, Q.; Luo, Y.; Li, J.; Feng, D.; Zhang, J.; Wu, Z.; Xu, H. Extraction, Purification, and Antioxidant Activity of Exopolysaccharides Produced by *Lactobacillus kimchi* SR8 from Sour Meat in Vitro and in Vivo. *CYTA—J. Food* **2021**, *19*, 228–237. [[CrossRef](#)]
89. Pan, D.; Mei, X. Antioxidant Activity of an Exopolysaccharide Purified from *Lactococcus lactis* Subsp. *lactis* 12. *Carbohydr. Polym.* **2010**, *80*, 908–914. [[CrossRef](#)]
90. Zhao, W.; Zhang, J.; Jiang, Y.Y.; Zhao, X.; Hao, X.N.; Li, L.; Yang, Z.N. Characterization and Antioxidant Activity of the Exopolysaccharide Produced by *Bacillus amyloliquefaciens* GSBa-1. *J. Microbiol. Biotechnol.* **2018**, *28*, 1282–1292. [[CrossRef](#)]
91. Gulcin, I.; Alwasel, S.H. Metal Ions, Metal Chelators and Metal Chelating Assay As. *Processes* **2022**, *10*, 312. [[CrossRef](#)]
92. Abdalla, A.K.; Ayyash, M.M.; Olaimat, A.N.; Osaili, T.M. Exopolysaccharides as Antimicrobial Agents: Mechanism and Spectrum of Activity. *Front. Microbiol.* **2021**, *12*, 664395. [[CrossRef](#)] [[PubMed](#)]
93. He, F.; Yang, Y.; Yang, G.; Yu, L. Studies on Antibacterial Activity and Antibacterial Mechanism of a Novel Polysaccharide from *Streptomyces virginia* H03. *Food Control* **2010**, *21*, 1257–1262. [[CrossRef](#)]

Disclaimer/Publisher’s Note: The statements, opinions and data contained in all publications are solely those of the individual author(s) and contributor(s) and not of MDPI and/or the editor(s). MDPI and/or the editor(s) disclaim responsibility for any injury to people or property resulting from any ideas, methods, instructions or products referred to in the content.